MASTERARBEIT | MASTER'S THESIS

Titel | Title

Influence of Int1 and the repeat clusters on the inversion of the central region of PhiCh1

verfasst von | submitted by

Clara Beer BSc

angestrebter akademischer Grad | in partial fulfilment of the requirements for the degree of

Master of Science (MSc)

Wien | Vienna, 2024

Studienkennzahl lt. Studienblatt | Degree programme code as it appears on the student record sheet:	UA 066 830
Studienrichtung lt. Studienblatt | Degree programme as it appears on the student record sheet:	Masterstudium Molecular Microbiology, Microbial Ecology and Immunobiology
Betreut von | Supervisor:	ao. Univ.-Prof. Dipl.-Biol. Dr. Angela Witte

Acknowledgements

My first and foremost thanks go to my supervisor Ao. Univ.-Prof. Dipl.-Biol. Dr. Angela Witte for her incredible support regarding all matters big and small. She taught me many lessons both for my life inside and outside the lab and I am eternally grateful for all the laughs we shared. The work in her lab was truly a special and shaping time for me as Angela is not only an amazing scientist but also a wonderful person.

I am also deeply grateful for my colleagues, especially Anna, Gregor, Ermirë and Benni without whom the time would have neither been this productive nor this fun. Thank you for all your support, all the drinks and all the awesome adventures.

I would also like to thank the Moll and Bläsi groups, especially Elisa and Denise for all the talks and coffees which we shared. They always had the right advice for me.

And last but not least, I am truly thankful for Fotima Touraeva and Isabel Del Pino Gomez for all the vital work they did and keep on doing.

Abstract

The temperate head-tail virus ϕCh1 harbors repeat clusters (ORF34, ORF36) and an invertase (*int1*) in the central region of its genome. The inversion of the 3' ends of ORF34 and ORF36 leads to the expression of a recombined protein $gp34_{52}$ which in turn is involved in the infection of *N. magadii*, its only known host.

To further investigate this inversion reaction, two different plasmids were cloned into *N. magadii* L13, a strain cured of the virus, containing either ORF34, *int1* and ORF36 or only ORF34 and ORF36. Growth curve samples were analyzed via PCR. As polymerases are known to be unreliable when amplifying repetitive sequences and the results differed greatly from previous ones achieved with a now unavailable polymerase, no concrete conclusions could be drawn.

Furthermore, *int1* deletion mutants were produced through deletion plasmids. The deletion was confirmed via PCR and Southern Blot followed by plaque assays and Western Blots. The two investigated mutants showed different infectivities as one clone presumably carries ORF34 in its unrecombined form and the other in its recombined form. Due to PCR inaccuracies, it was not possible to classify the clones without doubt. The Western Blot of both showed a signal for the recombined $gp34_{52}$ but the used antibody could previously not distinguish between gp34 and gp36. Therefore, further investigations are needed.

Moreover, a deletion plasmid of ORF36 in its reverse orientation was constructed to produce a ΔORF36 mutant. So far no positive clones were obtained.

Contents

Introduction

Archaea

Almost 50 years after being recognized as the third domain of life, Archaea still remain both the most enigmatic domain as well as the domain most defined by chronic energy stress or rather their ability to withstand and adapt to it (Valentine, 2007).

Currently, Archaea are divided into three superphyla: the Asgard-, DPANN- and TACK-Archaea with the *Euryarchaeota* not belonging to any of the three (Baker et al., 2020; Woese et al., 1990). Cultivated Archaea can be divided into six broad physiological (halophiles, thermophiles, acidophiles and anaerobic methane oxidizers) or metabolic (nitrifiers and methanogens) groups. It has been proposed that chronic stress is the crucial factor distinguishing Archaea from Bacteria (Valentine, 2007) but first the question arises: What are the similarities between Bacteria, Eukarya and Archaea?

At the first glance, Archaea and Bacteria seem highly similar, at least regarding their general cellular organization as both are unicellular and lack a nucleus as well as organelles (Fig. 1). Interestingly, on the second glance the cellular machinery is more closely related to eukaryotes as their DNA replication, transcription and translation are similar. Finally, Archaea share a set of unique cellular hallmarks like their membrane structure, their mobility apparatus as well as unique types of metabolism, like methanogenesis (Tomkins, 2015; Valentine, 2007; van Wolferen M, 2022; Albers SV, 2015; Albers SV, 2018; Lyu Z, 2018).

Trait	Bacteria	Archaea	Eukarya
Carbon linkage of lipids	Ester	*Ether*	Ester
Phosphate backbone of lipids	Glycerol-3-phosphate	*Glycerol-1-phosphate*	Glycerol-3-phosphate
Metabolism	Bacterial	Bacterial-like	Eukaryotic
Nucleus	No	No	Yes
Organelles	No	No	Yes
Spliceosomal introns	No	No	Yes
Telomeres	No	No	Yes
Chromosome shape	Mostly circular	Circular	Linear
DNA replication	Bacterial	Eukaryotic-like	Eukaryotic
Transcription	Bacterial	Eukaryotic-like	Eukaryotic
Translation	Bacterial	Eukaryotic-like	Eukaryotic

Figure 1: Differences and similarities between Bacteria, Eukarya and Archaea (Tomkins, 2015)

As mentioned before, the chemical structure of lipids composing the cytoplasmic membrane is unique to Archaea and is thought integral in explaining their ability to thrive in extreme conditions.

Bacteria typically have fatty acids esterified to a glycerol moiety whereas archaeal lipids generally consist of isoprenoidal alcohols that are ether-linked to glycerol making archaeal membranes less permeable to ions. This in turn, reduces the amount of futile ion cycling to maintain the chemiosmotic potential which results in an energy advantage over Bacteria (Hulbert & Else, 2005; Macalady et al., 2004; Mathai et al., 2001; Valentine, 2007; Van De Vossenberg et al., 1998).

But the archaeal membranes are not the only adaption made for thriving in harsh environments. This will be further elucidated using the example of halophilic Archaea. Extremely halophilic organisms – halophilic Bacteria as well as Archaea are known – grow best in environments containing 2.5-5.2 M salt. These conditions are found most often in salt lakes or marine salterns but a halophilic archaeon has also been found in the thalassohaline Deep Lake in Antartika (Demaere et al., 2013; Falb M, 2008; Oren, 1994). Considering their environment, halophilic archaea are adapted to low water availability and high ionic strength which leads to the accumulation of inorganic ions – mostly KCl – in their cytoplasm. This in turn, requires adaption of the archaeal proteins to remain functional under such conditions which is achieved by a high content of acidic amino acids and a low amount of basic amino acids in their proteins (Falb et al., 2008; Fendrihan et al., 2006; Oren, 1994, 2002; Stan-Lotter & Fendrihan, 2015; Vreeland, 2012).

Natrialba magadii

Natrialba magadii was isolated 1980 from the Lake Magadi, a soda lake in Kenia which is still the only known habitat of this rod shaped, strictly aerobic archaeon. As a haloalkaliphilic organism, *N. magadii* needs both hypersaline and alkaline conditions, therefore growing optimally in environments with 3.5 M NaCl concentrations and a pH of 9.5. Its growth temperature ranges from 37-42°C and under these conditions a generation time of approximately 9 hours can be achieved in the logarithmic phase (Tindall et al., 1980). It is noteworthy, that *N. magadii* is polyploid containing up to 50 chromosomal copies (Breuert et al., 2006).

N. magadii is the host to the head-tailed virus ϕCh1 and for research two strains are available: *N. magadii* L11 containing the virus and *N. magadii* L13 which was cured of the virus by repeated passaging (Witte et al., 1997).

There are limited model systems and genetic engineering tools available for Archaea contributing further to the challenges in researching this enigmatic third domain of life. For *N. magadii* a transformational system was developed and two shuttle vectors pRo-5 and pNB102 are currently available (Mayrhofer-Iro et al., 2013). The vector pRo-5 (Mayrhofer-Iro et al., 2013) contains operon ORF53/ORF54 (*repH*) of ϕCh1 as origin of replication (*ori*) as well as an ampicillin and novobiocin resistance. The second shuttle vector, pNB102, is based on a plasmid isolated from the

haloalkaliphilic archaeon *Natronobacterium sp*. strain AS7091 and contains an ampicillin and mevinolin resistance as well as the ColE1 *ori* in addition (Zhou et al., 2004).

Archaeal Viruses

Morphology

So far, 17 archaeal virus families with highly distinct morphologies have been identified which range from virions similar to head-tailed bacteriophages of the order *Caudovirales* to a multitude of archaea-specific virus morphotypes including bottle-shaped, coil-shaped and lemon-shaped particles (Krupovic et al., 2018; Luk et al., 2014; Munson-McGee et al., 2018; Pietilä et al., 2014; Prangishvili et al., 2017).

Interestingly, to date all isolated archaeal viruses have genomes comprised of DNA – in most cases linear or circular dsDNA – but in a few cases ssDNA genomes were found (Prangishvili et al., 2017). Forterre speculates that as no RNA archaeal viruses have been described so far they simply might not exist due to the last archaeal common ancestor potentially existing in a hyperthermophilic environment. Long RNA molecules are known to be extracellularly instable at high temperatures and therefore RNA archaeal viruses might have never evolved. Though Forterre reasons further that RNA archaeal viruses might still be discovered in the future (Forterre, 2013).

Attachment and virus entry

The attachment and virus entry for most archaeal viruses remains enigmatic but there are a number of exceptions. For example, filamentous viruses have been frequently observed to be bound through their ends to cellular appendages. This has been interpreted as the primary stage of virus-host interactions (Bettstetter et al., 2003; Prangishvili et al., 1999; Quemin et al., 2013).

In contrast, both the spindle-shaped virions of *Fuselloviridae* and *Bicaudaviridae* have been found to bind to cellular fragments or membrane-derived vesicles instead of cellular appendages. The attachment of *Sulfolobus monocaudavirus 1* (SMV1) has been studied in more detail by transmission electron microscopy (TEM) and three distinct attachment modes were discovered which might occur sequentially (Uldahl et al., 2016).

Firstly, the virion attaches to host cell via its nose-like end. Secondly, the virion aligns along the host cell and the main body is absorbed along the surface of the host while the tail remains unabsorbed. Thirdly, the virion's spindle morphology "disappears" as it seems to flatten against the host cell surface. This taken together with the lipid component of the SMV1 virion suggest a possible fusion entry mechanism but further studies are needed to substantiate this hypothesis (Uldahl et al., 2016).

The third attachment mechanism investigated to date is mediated by the tail of head-tailed viruses seemingly in a similar fashion to the mechanism employed by *Caudovirales* bacterial viruses. The importance of the virion tail fiber has been demonstrated for the myovirus ϕCh1 which infects *N. magadii*. Interestingly, ϕCh1 has been found to harbor a putative phase-variation system which results in the inversion of the ORF coding for the tail fiber protein therefore enabling infection (Klein et al., 2012; Rössler et al., 2004).

Egress mechanisms

Archaeal viruses are sometimes divided into two groups: one group resembles bacteriophages and carries multiple homologous genes while the other is archaeal-specific and for the most part does not share recognizable homologues (Krupovic et al., 2018; Pietilä et al., 2014). Generally, three different egress strategies have been found so far: firstly via virus-associated pyramids (VAPs), secondly via budding and thirdly via proteolytic cell lysis.

The formation of VAPs and its subsequent release of virions has so far only been observed in archaeal viruses and is the most extensively studied egress mechanism among the three. VAPs are pyramidal structures growing from the host cell membrane outwards. At the end of the infection cycle they protrude the S-layer to form apertures through which the mature virions exit the cell. The empty host cell remains a stable structure. Therefore, more parameters then the optical density of the culture are needed for investigating the viral life cycle (Baquero et al., 2021; Bize et al., 2009; Brumfield et al., 2009; Daum et al., 2014; Quax et al., 2011; Svirskaitė et al., 2016).

The second mechanism, the egress via budding, has been reported for eukaryotic viruses as well. They are – similarly to many archaeal viruses – often encased by envelopes containing host-derived lipids. Generally, when exiting the cell via virus budding the integrity of the host cell is maintained as the viral core is enveloped in the cellular membrane, followed by a fission event from the host cell. This egress method allows for continuous virion production (Baquero et al., 2021; Liu et al., 2017; Quemin et al., 2016).

The third egress strategy is achieved through cell lysis and mainly employed by head-tailed viruses of Archaea of the order *Caudovirales*. The strategy in general is similar to that of bacterial viruses of the same order but the composition of the cell envelopes of the respective hosts is fundamentally different. Consequently, the components of the holin-endolysin system – responsible for the lysis of bacteriophage host cells – have not been identified in archaeal viruses yet (Altermann et al., 2018; Dyall-Smith et al., 2003; Klein et al., 2002; Tang et al., 2004).

Some insights have been gained about possible lysis mechanisms of viruses infecting *Methanobacteriales* as pseudomurein endopeptidases are encoded by the known viruses of methanogens. Enzymatic studies have established the *in vitro* functionality of three of these endopeptidases and therefore involvement of them in the lysis process has been suggested (Altermann et al., 2018; Kok et al., 2010).

ϕCh1

The head-tail virus ϕCh1 has only one known host, *N. magadii*, and as a temperate phage can integrate into its host chromosomal DNA with the cell lysis being growth-phase dependent. Through electron micrographs the virus was imaged and its total length approximated to 200 nm with the head accounting for 70 nm and the contractile tail for the remaining 130 nm. As the tail is contractible, the virus was assigned to the family *Myoviridae*. ϕCh1 is adapted to its host physiology as its infectivity was greatly reduced in salt concentrations below 2 M (Witte et al., 1997).

The complete sequence of ϕCh1 of around 60 kbp has been established and based on this, 98 ORFs have been assigned. Further investigation revealed three major organizational units: the left part comprising a cluster of genes coding for structural proteins and genes probably involved in virion morphogenesis; the central part harboring functions for replication, plasmid stabilization and regulation of gene expression; and the right part primarily composed of genes of unknown function with the exception of genes coding for DNA methylation and restriction (Klein et al., 2002). This overall architecture is highly reminiscent of the structure of well-documented tailed bacteriophages (Brüssow & Desiere, 2001).

Site-specific recombination in the ϕCh1 genome

Special attention has to be drawn towards ORF35 and its surrounding regions as it is presumed to code of a site-specific λ integrase (*int1*). ORF35 is flanked by two almost identical repeats and two regions comprised of highly conserved 30 bp direct repeats which are part of ORF34 and ORF36 (Fig. 2). These repeats are similar to tail-fiber proteins of bacteriophages (Klein et al., 2002).

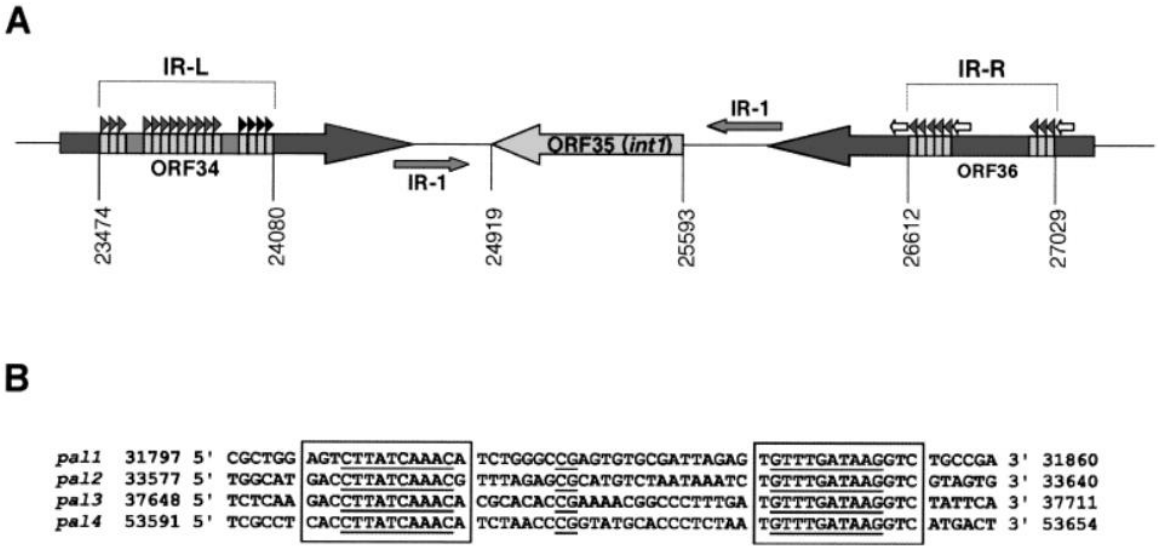

Figure 2: Physical map of the genome region embedding ORF35 and putative Int binding sites.
A. ORF35 (int1), the repeated elements IR-1, IR-L, IR-R as well as ORFs 34, 35 and 36 are indicated. The individual 30 bp direct repeats located within the repeat clusters IR-L and IR-R are represented by small arrowheads. Sequences with sequence similarities to each other located within or flanking IR-R are drawn as white arrows. Numbers indicate the positions of the respective elements within the ϕCh1 nucleotide sequence.
B. Nucleic acid sequence alignment of the putative ϕCh1 Int binding sites. The inverted repeats flanking the core region are boxed, and the nucleotides conserved within the four sites are underlined. Numbers indicate the start and stop positions of the sequence elements within the sequence of the ϕCh1 genome (adapted from Klein et al., 2002).

Further experiments revealed the presence of small circular molecules, the likely result of inversion and excision events. These inversion events resulted in the exchange of the 3' ends of ORF34 and 36 as they are in inverse orientation to each other. Through restriction analysis and sequencing, several different clones were revealed (Fig. 3). They all showed complete identity at the 5' and 3' end but internal differences in the form of the number and position of the repeats. Two clones also showed the exchange of the 3' ends of ORF34 and ORF36 and the inverted orientation of ORF35. The clones were categorized via the orientation of ORF35: if ORF35 is in the inverted direction in respects to ORF34, it was designated as the + orientation, otherwise is was classified as the - orientation (Rössler et al., 2004).

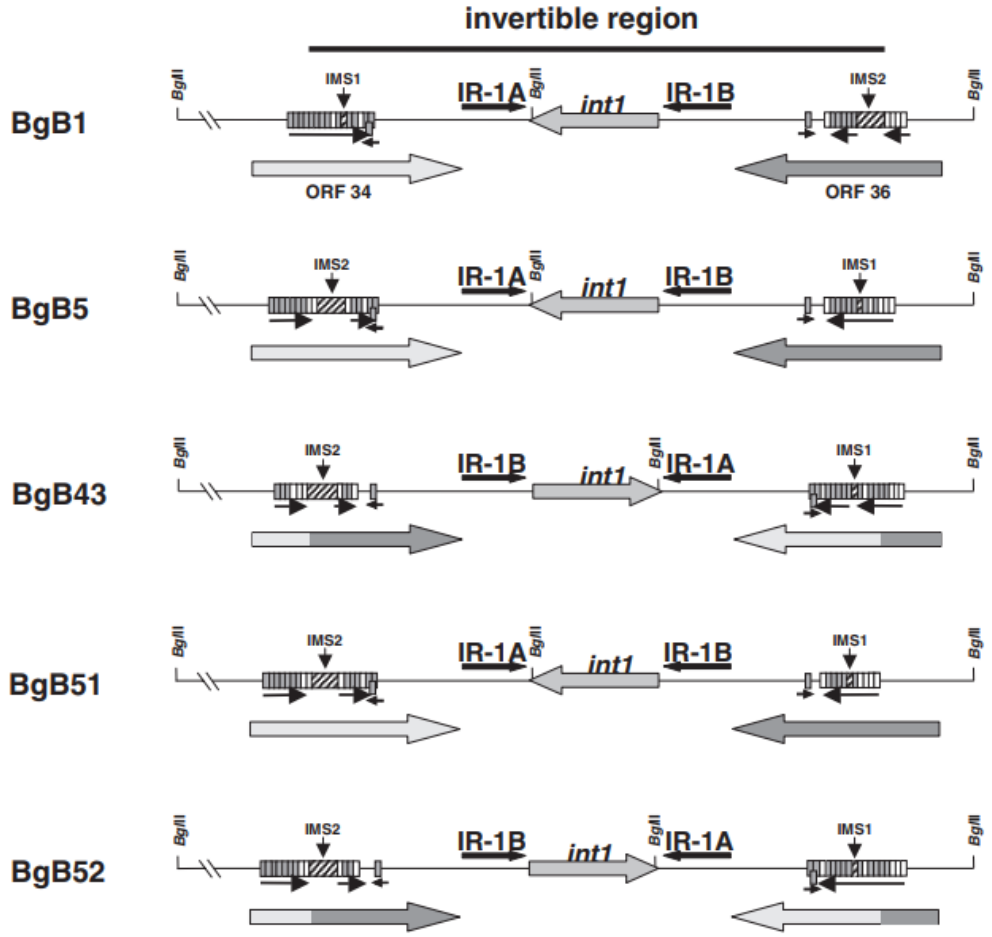

Figure 3: Variants found in ϕCh1: schematic representation of sequenced clones and specific effects on the C-terminal parts of ORFs 34 and 36.The int1 open reading frame is indicated as a large arrow, and the repeats found within the distinct clones are displayed as small boxes. Repeats containing the conserved 5' end ATGGAcgC are indicated in grey, and repeats with mismatches within this sequence are marked with white boxes. Small black arrows indicate the orientation of the repeats. Overlapping, reversed repeats within a cluster are drawn staggered and slightly lower with respect to the others. Above clone Bgb1, the invertible region is marked with a line. Two other sequences within the repeat clusters are marked with white boxes containing inclined lines: the 207-bp-long intermediate sequence 2 (IMS2), which is identical in all clones independent of the different inverted repeats, as well as the 33-bp-long intermediate sequence 1 (IMS1), again identical in all clones. Diagonal slashes on the left indicate regions that are not indicated in the representation. Large arrows below the repeat clusters indicate the composition of ORF34 and ORF36 as well as their variants. The BglII restriction sites are indicated. Adapted from Rössler et al., 2004.

Previous antiserum raised against $gp36_1$ could not distinguish between gp34 and gp36, therefore two new approaches were used: firstly, the transcription of ORF34 and ORF36 was analyzed via PCR and secondly, plasmids containing $ORF34_1$ and $ORF36_1$ and their upstream regions were transformed into *H. volcanii* (Klein et al., 2012).

The transcription of ORF34 and 36 was monitored using primers specific for BgB1-type ORF34 and 36 (+ orientation) and BgB52-type ORF34 and 36 (- orientation). For both approaches PCR products for $ORF34_1$ and $ORF34_{52}$ were obtained upon transition in the late logarithmic growth phase and onset of lysis. Transcription was neither for $ORF36_1$ nor for $ORF36_{52}$ detected (Klein et al., 2012).

The results for a transformation experiment followed by a Western Blot detection were similar: Only $ORF34_1$ was able to express a protein which was then recognized by $\alpha-\phi$Ch1 antiserum. Therefore, it was concluded that only ORF34 codes for a protein (Klein et al., 2012).

Furthermore, the time kinetics of the inversion reaction were investigated via PCR as well. $ORF34_1$ was detected throughout the entire life cycle of strain L11 whereas $ORF34_{52}$ was absent on days 1 and 2 but appeared in later samples. This indicates that an inversion had occurred during this period of time (Klein et al., 2012).

As putative tail fiber proteins, $ORF34_1$ and $ORF34_{52}$ were further investigated and their sequences revealed similarities to galactose-binding domains. Notably, only $ORF34_{52}$ had the conserved amino acids sequence, which is known to form the binding pocket for α-D-galactose. Therefore, $ORF34_1$ and $ORF34_{52}$ were expressed in *H. volcanii* and their crude extracts incubated with L13. After centrifugation, $gp34_1$ was exclusively found in the cell supernatant, whereas $gp34_{52}$ was exclusively found in the pellet fraction, suggesting that only $gp34_{52}$ is able to bind to *N. magadii* cells (Klein et al., 2012).

To collect stronger evidence, the experiment was repeated with proteins expressed in *E. coli* yielding the same results. Truncated versions of $gp34_{52}$ were investigated as well. Only the proteins containing the C-terminus were able to bind to *N. magadii* and lost their binding ability if a conserved amino acid inside the binding domain was modified (Klein et al., 2012).

Taken together, ORF34 seems to be part of a phase-variation system yielding distinct versions of the tail fiber protein with different binding and therefore different infectivity properties (Klein et al., 2012).

Further experiments were conducted, in which a plasmid containing *int1* and two single repeats separated by spacer sequence were introduced into *E. coli*. On one plasmid the repeats were in direct orientation to each other and no inversion reaction could be observed. The other plasmid had them in inversed orientation for which an inversion was detected (Ladurner, 2008).

As a next step, two plasmids were cloned into *N. magadii* L13: firstly, the plasmid pRo-5 52-2 containing $ORF34_{52}$, ORF35 and $ORF36_{52}$ and secondly the plasmid pRo-5 52-3 containing $ORF34_{52}$ and $ORF36_{52}$ without ORF35.

The inversion reaction was detectable for pRo-5 52-2 after 78 hours whereas no inversion specific PCR product was obtained for pRo-5 52-3. Therefore, Int1 seems to be responsible for the inversion reaction between the indirect repeat sequences. Interestingly, Klein et al. detected the expression of *int1* in early logarithmic growth phase whereas the inversion was first observed in the stationary

growth phase. This difference between the expression and the inversion could point towards the involvement of a second protein (Klein et al., 2012; Ladurner, 2008).

Thesis Aim

The aim of this thesis was to further the understanding of ORF34, ORF35 (*int1*) and ORF36. Therefore, a plasmid containing ORF34, ORF35 and ORF36 was cloned into *N. magadii* L13, the cured strain. Possible inversion events were monitored throughout the growth phase and compared to *N. magadii* L13 containing a plasmid carrying only ORF34 and ORF36.

Furthermore, a deletion plasmid of ORF35 was cloned into L11 in order to delete *int1*. The deletion was confirmed via PCR and Southern Blot. The inversion events were investigated via the infectivity of the *int1* knock out mutants through plaque assays and compared to the infectivity of the wild type L11. The presence of $gp34_1$ was also detected through Western Blots.

Finally, a deletion plasmid of ORF36 in its reverse form was designed through Gibson Assembly and cloned into L11 to produce a ΔORF36 mutant.

Material and Methods

Materials

Bacterial and archaeal strains

Escherichia coli

Strain	Modifications	Source
XL1-Blue	endA1, gyrA96, hsdR17 (rk-mK+), lac, recA1, relA1, supE44, thi-1, [F´, lacIq , lacZΔM15, proAB+, Tn10 (TetR)]	Stratagene

Natrialba magadii

Strain	Modifications	Source
L11	contains wild type ϕCh1	Witte et al., 1998
L11 ΔORF35	ORF35 of ϕCh1 has been deleted	this study
L11 ΔORF36	ORF36 of ϕCh1 has been deleted	this study
L13	cured from ϕCh1	Witte et al., 1998
L13 (pRo-5 52-2)	contains plasmid with ϕCh1 ORF34-36	Ladurner, 2008
L13 (pRo-5 52-3)	contains plasmid with ϕCh1 ORF34 and ORF36	Ladurner, 2008

Growth media

E. coli

Lysogeny broth medium (LB) for *E. coli*

NaCl	5 g
Yeast extract	5 g
Peptone	10 g

pH 7.0

dH_2O ad 1 l

15 g/l agar for plates

N. magadii

NVM-CAA+/ NVM-CH+

NaCl	235 g
KCl	2.4 g
yeast extract	11.7 g
casamino acids (CAA)/ casein hydrolysate (CH)	8.8 g
sodium citrate tribasic dehydrate	0.8 g

pH 9-9.5 with NaOH

ddH_2O ad 935 ml

for plates: 10 g/l agar

autoclave

After autoclaving complemented with:

0.57 M Na_2CO_3 (dissolved in sterile ddH_2O)	63 ml
1 M $MgSO_4$ (autoclaved)	1 ml
20 mM $FeSO_4$ (dissolved in sterile ddH_2O)	1 ml
trace elements SL-6	1 ml

1000x Trace Elements SL-6

$CoCl_2$ * 6 H_2O	0.2 g
$CuCl_2$ * 6 H_2O	10 mg
H_3BO_3	0.3 g
$MnCl_3$ * 4 H_2O	30 mg
Na_2MoO * 4 H_2O	30 mg
$NiCl_2$ * H_2O	20 mg
$ZnSO_4$ * 7 H_2O	0.1 g

pH 3-4 with HCl

dH_2O ad 1000 ml

sterilized by filtration

Additives

Compound	Stock concentration	Final Concentration	Preparation
Ampicillin	20 mg/ml	100 µg/ml	dissolved in dH_2O, sterile filtered, stored at 4°C
Tetracycline	10 mg/ml	10 µg/ml	dissolved in half of EtOH and half dH_2O, stored at -20 °C
Novobiocin	3 mg/ml	3 µg/ml	dissolved in dH_2O, sterile filtered, stored at -20 °C
Bacitracin	7 mg/ml	70 µg/ml	dissolved in dH_2O, sterile filtered, stored at 4°C

Plasmids

Plasmids	Features	Source
pRo-5 52-2	ϕCh1 ORF34 - 36	Ladurner, 2008
pRo-5 52-3	ϕCh1 ORF34 and 36	Ladurner, 2008
ΔORF35	deletion plasmid for deletion of ϕCh1 ORF35 in L11	Schülein, 2019
ΔORF36	deletion plasmid for deletion of ϕCh1 ORF36 in L11	this study

Primers

Name	Sequence
Int-Flag-5	GACGCGTGGCATATGTCCAAAGAGAGACATGCCCA
Int-Flag-3	AACGAAGGAAAGCTTGGCGCGATCAGCCGTAG
34-5	CAGCAGAGATCTATGAGTAAATCTGGGAACCGAG

34-3	CAGCAGAAGCTTCAGATCAGGTTTATATTGCTGAAGT
36-5	GACGACAGATCTATGGATCCGATCAGCGTG
36-3	CAGCAGAAGCTTATTCAGGTTTCATGTCGCTG
40-5	CAGCCGGATCCATGTGCTGGATGAGCATCTAC
34-D-5	CAGGAGATCTATGCCGCGAAGTGCG
36-D-5	GACGGGATCCATGGCGGTCGGGAAGT
Nov-9	GATGTCGGTCATCGCGG
Nov-12	GCCGGTGAGTACTTAACGC
Int-3-C	GTTCATCGATTCAGCCGTAGATCTCGAG
DInt1-5en	GACCGTTCCATACTCCAGC
DInt1-3en	GTGGTACCCACGACGTACTGTTC
DORF36-2-3	ATCCCCCGGGCTGCAGGAATTCGATAACCAATGCAACTGATCTTCACACC
DORF36-4-2	GGTCGACGGTATCGATAAGCTTGATTCACTGCGGAGCCTTCAACCACTCA
D36R-3en	ACATGCCCACGAAGACGC
D36F-3en	GTCTTCGTGGGCATGTCTCTC
TP3	CAGCGGATCCATGGAACTCATTTTCACACCG
TP4	GACTAAGCTTCCATTTATTCGTTGCTACGAGT
DORF36-1	ATCCCCCGGGCTGCAGGAATTCGATTCAGCCGTAGATCTCGAGTAGAGCT
DORF36-5R	TCGTTCCAGTCGACACTGCAGGATCATGTCCAAAGAGAGACATGCCCACG
DORF36-6R	AGCTGGATATTACGGCCCGGGTAACAACTAACCCAGAAACCCACAACCAG
DORF36-7R	GGTCGACGGTATCGATAAGCTTGATTCACTGCGGAGCCTTCAACCACTCA
NovR-1p	GATCCTGCAGTGTCGACTGGAACGAGG
NovR-2s	GTTACCCGGGCCGTAATATCCAGCTGA
36-en-5	GTACGACTTCAGGAGCTCGTCG

36-en-3	GTCGCGTGACGCTGTC
DORF36-del1	GCGAGATCGTCTTCGACG
DORF36-del2	GTGCAACTGCGGTCTGTACG

Kits

Name	**Usage**	**Manufacturer**	**Product Number**
Promega Wizard® SV Gel and PCR Clean-Up System	Purification of gel eluted DNA fragments and PCR products	Promega	A9281
Wizard® Plus SV Minipreps DNA Purification System	Isolation of plasmid DNA from *E. coli*	Promega	A1460
Chemiluminescent Nucleic Acid Detection Module	Imaging of Southern Blot	Thermo Scientific	89880

Enzymes

Enyzme Name	**Manufacturer**	**Product Number**
2x*GoTaq* Green Master Mix	Promega	M7122
Phusion Flash PCR Master Mix	Thermo Scientific	F548S
Vent (exo-) DNA Polymerase	New England BioLabs	M0257S
Pwo DNA Polymerase	Roche	11644955001
Pfu DNA Polymerase	Promega	M7745
*Pvu*II-*HF*	New England BioLabs	R3151S
Fast AP Alkaline Phosphatase	Thermo Scientific	EF0652
Proteinase *K*	Qiagen	Lot. No. 160020092 Mat No. 1019499

Size Markers

Marker	Manufacturer	Product Number	Fragments [kDa]/[bp]
PageRuler™ Plus Prestained Protein Ladder, 10 bis 250 kDa	Thermo Scientific	26619	**~10**, ~15, **~25**, ~35, ~55, **~70**, ~100, ~130, ~250
GeneRuler 1 kb DNA Ladder	Thermo Scientific	SM0311	250, 500, 750, **1000**, 1500, 2000, 2500, **3000**, 3500, 4000, 5000, **6000**, 8000, 10000
GeneRuler 1 kb Plus DNA Ladder	Thermo Scientific	SM1331	75, 200, 300, 400, **500**, 700, 1000, **1500**, 2000, 3000, 4000, **5000**, 7000, 10000, 20000

Antibodies

Primary Antibody

Antibody	Target	Application	Source
α-gp34$_{52}$ (rabbit #20)	ϕCh1 gp34	Diluted 1:2500 in 1x TBS, 0.3% BSA, 0.02% NaN_3	Till (2011)

Secondary Antibody

Antibody	Target	Application	Source
ECL™ Anti-Rabbit IgG, Horseradish peroxidase linked whole antibody (from donkey) Lot 17434242 NA934V	Rabbit IgG	Diluted 1:5000 in 1x TBS	GE Healthcare

SDS-Polyacrylamid gels

Compound	12% Separating Gel	4% Stacking gel
Acrylamide solution 30%	2 ml	267 µl
Separating Gel Buffer	1.25 ml	-
Stacking Gel Buffer	-	0.5 ml
dH_2O	1.75 ml	1.233 ml
APS 10 %	60 µl	20 µl
TEMED	10 µl	5 µl
Total Volume	5 ml	2 ml

Membrane

For the Western Blots, the Nitrocellulose Blotting Membrane Amersham Protean 0.2 µm GE Healthcare Life Science (Catalogue Number 10600001) was used.

General Buffers and Solutions

Buffers for DNA methods

General

50x TAE

Tris-HCl pH 8.2	2 M
acetic acid	1 M
EDTA	0.1 M

50x Super Buffer

NaOH	0.5 M
boric acid	1.82 M

6x DNA loading dye

orange G	0.144% m/v
xylene cyanol	0.036% m/v
Tris-HCl pH 8.0	0.025 M
glycerol	60 %

Ethidiumbromide bath

ethidiumbromide	10 µg/ml

Southern Blot

Denaturation Solution

NaOH	0.4 M
NaCl	0.6 M

Neutralization Solution

NaCl	1.5 M
Tris-HCl pH 7.5	0.6 M

20x SSC solution

NaCl	3 M
Sodium citrate	0.6 M

adjust to pH 7.2 with HCl

Hybridization buffer

ddH_2O	55 ml
20x SSC	25 ml
50x Denhardt's Solution	10 ml
10% BSA	5 ml
1M Na_2HPO_4	5 ml
20% SDS	500 µl
0.5 M EDTA	200 µl

Washing Solution I (2x SSC/ 0.1% SDS)

20x SSC	50 ml
20% SDS	2.5 ml
ddH_2O	447.5 ml

Washing Solution II (0.1x SSC/ 0.1% SDS)

20x SSC	2.5 ml
20% SDS	2.5 ml
ddH_2O	495 ml

Buffers for protein methods

10x SDS-running buffer

tris base	0.25 M
glycine	1.92 M
SDS	1 %

4x Stacking gel buffer

Tris-HCl pH 6.8	0.5 M
SDS	0.4 %
autoclaved	

4x Separating gel buffer

Tris-HCl pH 8.8	1.5 M
SDS	0.4 %
autoclaved	

10 % APS

ammonium persulphate	1 g
dH_2O ad 10 ml	
stored at 4°C	

2x Laemmli sample buffer

Tris-HCl pH 6.8	0.12 mM
SDS	2 %
Glycerol	17.4 %
β-mercaptoethanol	2 %
bromphenolblue	0.02 %

100 ml Na-Phosphate buffer pH 6.8

1 M Na_2HPO_4	46.4 ml

1 M NaH_2PO_4	53.7 ml

Coomassie staining solution

Methanol	40 %
acetic acid	10 %
coomassie Brilliant Blue R-250	0.25 %

Coomassie destaining solution

acetic acid	10 %

Blocking solution

Milk powder	5 %
in 1x TBS	

10x TBS

Tris-HCl pH 8.0	0.25 M
NaCl	1.37 M
KCl	27 mM

1x Towbin transfer buffer

Methanol	20% v/v
tris base	25 mM
glycine	192 mM

ECL buffer

1.5 M Tris pH 8.5	13.3 ml
1 aliquot Luminol	500 µl
1 aliquot Coumaric acid	250 µl

ad 200 ml dH_2O

stored at 4°C, protected from light

Coumaric acid

Coumaric acid	0.148 g
DMSO	10 ml

250 µl aliquots stored at -20 °C

Luminol

3-Aminophthalthydrazide	0.886 g
DMSO	20 ml

500 µl aliquots stored at -20 °C protected from light

Buffers for E. coli *methods*

MOPS I

MOPS	100 mM
$CaCl_2$	10 mM
RbCl	10 mM

pH adjusted to 7.0 with KOH

MOPS II

MOPS	100 mM
$CaCl_2$	70 mM
RbCl	10 mM

pH adjusted to 6.5 with KOH

MOPS IIa

MOPS	100 mM
$CaCl_2$	70 mM
RbCl	10 mM
Glycerol	15 %

pH adjusted to 6.5 with KOH

***E. coli* glycerol**

Glycerol	80 % v/v

in H_2O; autoclaved

Buffers for N. magadii *methods*

Buffered high salt spheroplast solution

Tris/HCl pH 9.5	50 mM
NaCl	2 M
KCl	27 mM

after autoclaving, 15 % sucrose (sterile filtered) are added

60 % PEG 600

PEG-600*	60 % v/v

UBSS-HS	40 % v/v

*PEG-600 aliquots of 600µl are stored at -80°C for a maximum duration of six months

Unbuffered high salt spheroplast solution UBSS-HS

NaCl	2 M
KCl	27 mM

after autoclaving, 15 % sucrose (sterile filtered) are added

Gibson Assembly Master Mix

5x ISO reaction buffer

PEG-8000 (25 % w/v)	2.5 g
1 M Tris-HCl, pH 7.5 (500 mM)	5 ml
1 M $MgCl_2$ (50 mM)	500 µl
DL-Dithiothreitol (50 mM)	77 mg
100 mM dATP (1 mM)	100 µl
100 mM dGTP (1 mM)	100 µl
100 mM dCTP (1 mM)	100 µl
100 mM dTTP (1 mM)	100 µl
NAD (5 mM)	33.2 mg
Nuclease-free water	ad 10 ml

Self-made Gibson Assembly Master mix

5x ISO reaction buffer	100 µl
T5 Exonuclease [10U/µl] (NEB M0363S)	0.2 µl
Phusion polymerase [2 U/µl] (NEB M0530S)	6.25 µl

Taq DNA ligase [40 U/µl] (NEB M0208S)	50 µl
Nuclease-free water	218.55 µl

Virus isolation

Dialysis Solution

NaCl	4 M
Tris-HCl pH 9.5	50 mM

CsCl Gradient: Solution 1.1

CsCl	20 g
NaCl	23.4 g
Tris-HCl pH 9.5	50 mM

CsCl Gradient: Solution 1.3

CsCl	90 g
NaCl	23.4 g
Tris-HCl pH 9.5	50 mM

CsCl Gradient: Solution 1.5

CsCl	135 g
NaCl	23.4 g
Tris-HCl pH 9.5	50 mM

Methods

DNA methods

Agarose gel electrophoresis and staining

DNA fragments were separated in 0.8 % agarose gel with 1x TAE (fragment >1 kbp) or 1x Super Buffer (fragments up to 1500 bp). Afterwards the gels were stained with ethidium bromide (10 µg/ml in dH_2O).

Preparative PCR

Thermo Scientific *Phusion* Flash High-Fidelity PCR Master Mix was used for preparative PCRs.

Components	**Amount [µl]**
Phusion Flash Master Mix High-Fidelity	25
ddH_2O	19
Primer 1 (0.1 µg/µl)	2.5
Primer 2 (0.1 µg/µl)	2.5
DNA template (~50-100 ng)	1
Total volume	50

The following *Phusion* Flash Master Mix High-Fidelity PCR program was used.

Step	**Temperature [°C]**	**Time [mm:ss]**
1 Initial Denaturation	98	05:00
2 Denaturation	98	00:15
3 Annealing	T_m primer - 5°C	00:15
4 Elongation	72	15 s/ 1 kbp
5 Final Elongation	72	3x elongation time
6 Hold	4	∞

Steps 2-4 were repeated 34 times.

Analytical PCR

Promega *GoTaq* Green Master Mix was used for analytical PCRs.

Components	**Amount [µl]**
2x*GoTaq* Green Master Mix	12.5
ddH_2O	8.5
Primer 1 (0.1 µg/µl)	1.5
Primer 2 (0.1 µg/µl)	1.5
DNA Template (~50-100 ng)	1
Total volume	25

1µl of *E. coli* culture was used directly as template. In order to use *N. magadii* culture as template, 30 µl of culture were centrifuged at 13 500 rpm for 3 min. The supernatant was removed and the pellet resuspended in 100 µl ddH_2O.

The following *GoTaq Green Master Mix* PCR program was used:

Step	**Temperature [°C]**	**Time [mm:ss]**
1 Initial Denaturation	98	05:00
2 Denaturation	98	00:15
3 Annealing	T_m primer - 5°C	00:15
4 Elongation	72	1 min/ 1 kbp
5 Final Elongation	72	3x elongation time
6 Hold	4	∞

Steps 2-4 were repeated 24-34 times.

DNA gel elution

After vector restriction or preparative PCR for the Gibson Assembly, the desired band was isolated from an agarose gel using the "Promega Wizard® SV Gel and PCR Clean-Up System" according to manufacturer's protocol and eluted in 30 µl dH_2O.

DNA restriction

Restrictions were performed at 37 °C for at least 3 hours or overnight. Restriction enzymes provided by New England BioLabs were used in their recommended buffer.

Gibson Assembly

To ligate one or more fragments into a vector, Gibson assembly was performed. Therefore, the vector was linearized, mixed with a three- to five-fold molar excess of fragments (0.5 – 1 pmol per fragment) and added to 10 µl of Gibson assembly master mix followed by incubation at 50°C for 15-30 min. The reaction was shortly put on ice. Then, *E. coli* XL-1 Blue cells were transformed with 10 µl of the Gibson assembly mix.

Isolation of plasmid DNA

Plasmids were isolated from *E. coli* overnight cultures using the "Wizard® Plus SV Minipreps DNA Purification System" according to the manufacturer's protocol.

Southern Blot

Probe generation

Component	**Final volume [µl]**
2x *GoTaq* Green Master Mix	50
primer 1	10
primer 2	10
L11 wild type DNA	1
ddH_2O	26.5
biotinylated dUTP (1:4 dilution)	2.5
total	100

35 PCR cycles were used to generate both the 3' and 5' probes which were afterwards eluted from a 0.8% Super Buffer agarose gel in 30 µl ddH_2O. Before hybridization, they were denatured for 10 min at 95°C and afterwards immediately placed on ice.

Capillary Blot

The 3' and 5' probe were added to one membrane each with everything being done in duplicates.

The restricted L11 wild type DNA together with the restricted L11 ΔORF35 mutant DNA were separated by a 0.8% TAE agarose gel and stained with ethidium bromide. After imaging, the gel was first incubated in the denaturation solution for 30 min at RT and afterwards in the neutralizing solution for 30 min as well.

A capillary blot was built with a layering paper as the base with the gel on top of it, followed by the membrane, a stack of paper towels, a glass plate and a weight to fixate it. The DNA was transferred overnight followed by 1 min incubation in 0.4 M NaOH and 1 min in 0.2 M Tris-HCl pH 7.5. Subsequently, the DNA was fixed to the membrane via UV-crosslinking.

Prehybridization and hybridization

For blocking, the membrane was incubated in a hybridization flask with 12 ml hybridization buffer and 120 µl salmon sperm DNA (10 mg/ml) for 3 hours at 65°C. Afterwards, each denatured probe was added to one membrane and hybridized overnight at 65°C. Subsequently, the membrane was washed twice with washing solution I for 5 min at RT and twice with washing solution II for 15 min at 65°C.

Development and detection

The blot was developed according to the "Chemiluminescent Nucleic Acid Detection module" protocol. The hybridized DNA was detected by the Bio-Rad ChemiDoc Imaging System using the setting "High Sensitivity Chemiluminescence", with 5-180 s exposure time during which 30 pictures were taken.

Generation of competent cells and transformation procedure

Generation of competent E. coli *cells*

An overnight *E. coli* preculture was used to inoculate 200 ml LB medium containing tetracycline to an OD_{600} of 0.1. The culture was incubated at 37°C with agitation until an OD_{600} of 0.6-0.7 was reached. Upon reaching this point, the cells were harvested by centrifugation at 10 krpm for 10 min at 4 °C and afterwards the pellet was resuspended in 80 ml MOPS I and incubated on ice for 10 minutes. A second centrifugation step was performed followed by the resuspension of the

pellet in 80 ml MOPS II and a 30 min incubation on ice. After carrying out the third centrifugation step, the pellet was resuspended in 4 ml MOPS IIa and aliquoted in 100 µl to be stored at -80 °C.

Transformation of E. coli *competent cells*

After thawing the competent cell aliquot, DNA was added (10 µl Gibson assembly mix or up to 1 µg plasmid) and incubated on ice for 30 min followed by a heat shock for two minutes at 42°C after which the cells were immediately cooled on ice. 300 µl LB-medium were added and the cells were regenerated for 30 min at 37 °C. Subsequently, the cells were plated on selective medium and incubated at 37 °C overnight.

Single colonies were inoculated in 5 ml selective medium, incubated at 37 °C with agitation and directly used as template for analytical PCR screening. Plasmid DNA from positive clones was isolated and sent for sequencing (Microsynth).

E. coli *glycerol stock*

For longtime storage at -80 °C 1 ml of culture with an OD_{600} of 0.6-0.8 was mixed with 0.8 ml 50 % glycerol in a cryogenic vial (1.8 ml skirted cryovial with internal thread, silicone seal cap, star lab) and kept in the -80 °C freezer.

Transformation of N. magadii

Generation of competent *N. magadii* cells

A preculture of *N. magadii* was inoculated in 25 ml NVM CAA+ in a baffled flask and incubated at 42 °C with agitation to an OD_{600} >1. Of this preculture 4-6 ml were used to inoculate 50 ml of NVM-CAA+ containing bacitracin (70 µg/ml) in a baffled flask and were again incubated at 37 °C with agitation until an OD_{600} of 0.6 to 1 was reached. Cells were harvested by centrifugation at 6 krpm for 15 min at RT, followed by resuspension in 25-42 ml buffered high-salt spheroplasting solution depending on the OD_{600}. Proteinase K was added to a final concentration of 0.1 % v/v.

This cell suspension was incubated for approximately 48 hours at 42 °C with agitation until the cells lost their S-layer reflected in the formation of spheroplasts which was observed under the microscope. The competent cells were used and stored on RT for up to one week.

PEG-600 based Transformation of *N. magadii* cells

1.5 ml of competent cells were centrifuged for 3 minutes at 10 krpm at RT and the pellet was resuspended in 150 µl high salt buffered spheroplast solution. The DNA of interest was added and incubated 5 minutes at RT. For the transformation of common plasmids 1-3 µg of DNA in a volume of maximal 10 µl were used, for deletion plasmids 10-30 µg of DNA were used in a maximum of

10µl as well. 150 µl of 60 % PEG-600 (in HS unbuffered spheroplasting solution) were added to the transformation mix and incubated for 20 to 30 minutes at RT. Afterwards the cell mix was washed twice with 1 ml NVM CAA+ (10 krpm, 5 minutes, RT) to remove PEG-600 residues, then the final pellet was resuspended in 1 ml NVM CAA+ and incubated at 37 °C with agitation until cells regenerated their original rod shaped morphology, which took approximately two to three days.

Finally, 100 µl of the cell suspension (undiluted, 1:10 and 1:100 dilution for common plasmids, undiluted for suicide plasmids) were plated on NVM CAA+ agar plates with the corresponding antibiotics and incubated at 42 °C in sealed plastic bags to prevent desiccation of the plates. Single colonies were inoculated in 500 µl NVM CAA+ with the appropriate antibiotics and incubated at 37 °C with agitation followed by screening through analytical PCR.

Protein Methods

Crude extract protein sample for SDS-PAGE

Protein crude extract samples of *N. magadii* were taken daily for the duration of one week. 1.5 ml of culture were collected by centrifugation at 13 0000 rpm for 3 min, the supernatant was removed and a quick spin was performed to be able to take off any remaining supernatant. OD_{600} x 0.75 = µl 5 mM Na-PO_4 buffer (pH 6.8) were added to the pellet, and the pellet was scraped from the reaction tube. Afterwards, the same volume of 2x Laemmli buffer was added. If the added volume of 5 mM Na-PO_4 buffer and 2x Laemmli buffer would have been below 100 µl in total, another 1.5 ml of culture were used therefore doubling the added volumes. The mixture was incubated at 37 °C overnight to dissolve the pellet. Afterwards, protein crude extract samples were stored at -20 °C. Prior to loading the samples on an SDS-gel, the proteins were denatured at 95 °C for 10 min.

Western Blot

SDS-PAGE

For the Western Blot 8 µl of protein ladder and 7-14 µl of sample were loaded as determined by visual inspection of the Coomassie gel. As positive control *N. magadii* L11 (8 µl) and as negative control *N. magadii* L13 (8 µl) were loaded on each gel. Each gel was run at 40 V for approximately 4 hours.

Blotting, Blocking and Antibodies

Semi-dry blotting with Towbin transfer buffer was performed at 83 V for 20 min (2 gels) or 35 min (4 gels). Beforehand, membrane and Whatman filter paper were soaked in transfer buffer and stacked from the anode at the bottom to the cathode on top the following way: three Whatman papers, the membrane, the gel, three Whatman papers. A tube was carefully rolled over this

sandwich to remove air and excess liquid. After the transfer, the marker lines on the membrane were labelled with an indelible pen, for easier visualization later. The membrane was blocked overnight with 100 ml blocking solution at 4 °C with agitation. Subsequently, the membrane was washed three times for ten minutes with 1x TBS, followed by incubation with 10 ml of the primary antibody for one hour at room temperature and afterwards three washing steps. For the secondary antibody 10 ml 1x TBS and 2 µl of α-Anti-Rabbit coupled with Horseradish peroxidase were added to the membrane and incubated at room temperature for 1 h, after which the membrane was washed again three times with 1x TBS.

Detection

Right before detection 3 ml ECL and 2 µl H_2O_2 were added directly to the membrane, followed by tilting to cover the whole membrane evenly. Excess liquid was removed, the membrane placed inside the BioRad Chemidoc and detected using the setting "High Sensitivity Chemiluminescence", with 5-180 s exposure time during which 30 pictures were taken. Subsequently, a colorimetric picture was taken to merge with and visualize the marker.

Isolation of ϕCh1 virus particles

Three 1.5 l cultures of *N. magadii* (L11 wild type or ΔORF35) were incubated at 37°C, 165 rpm until complete lysis. Next, the cultures were centrifuged at 6 krpm for 15 minutes at RT. The supernatant was precipitated with 10% w/v PEG 6000 and stirred overnight at RT. After centrifugation at 6 krpm for 15 minutes at RT, the pellets were resuspended in 10 ml 4 M NaCl, 50 mM Tris-HCl pH 9.5 respectively. The next step was a discontinuous CsCl gradient ultracentrifugation. Therefore, 3 ml of 1.5 CsCl solution were overlayed with 4 ml of 1.3 CsCl solution. On top, 5 ml of the virus solution were added and the centrifugation tube was filled up completely with 1.1 CsCl solution. The gradient was centrifuged at 30 krpm for 20 hours at RT in the ultracentrifuge.

Afterwards, the virus particle band was isolated and mixed with 1.3 CsCl solution to be centrifuged again at 30 krpm for 20 hours at RT. As a final step, the virus particles were dialyzed against 4 M NaCl, 50 mM Tris-HCl pH 9.5 and stored at RT.

DNA isolation from ϕCh1 virus particles

400 µl dH_2O were added to 100 µl of the isolated virus particles and extracted at least 3 times using 250 µl phenol and 250 µl $ChCl_3$ until no interphase was visible. Then, 500 µl of $ChCl_3$ were added and the DNA was precipitated using 500 µl of isopropanol. This was followed by a centrifugation for 30 min at 18 000 rpm and 4°C. The pellet was washed twice with 1 ml of EtOH

and the DNA pellet was subsequently dried at 65°C. After the drying, the pellet was dissolved in 20 µl of dH_2O.

Virus methods

Virus titer analysis

Sampling

Samples for the analysis of the virus titer were taken daily for the duration of one week. 1.5 ml of the culture were centrifuged for 3 min at 13 000 rpm and RT. 1 ml of the supernatant was transferred into a fresh Eppendorf tube and 20 µl of $CHCl_3$ were added. The samples were stored at RT.

Virus titer analysis

The samples were serially diluted (10^{-2} , 10^{-4} , 10^{-6} , 10^{-8}) in NVM+ medium. 100 µl of each dilution was mixed with 500 µl of fresh *N. magadii* L13 culture in 5 ml NVM+ soft agar (56°C). This mixture was poured onto NVM+ plates which were dried overnight at RT and thereafter incubated at 37°C for one week in sealed plastic bags. Afterwards, the plaques were counted and the plaque forming units (PFU) calculated.

Virus adsorption into N. magadii *L13*

50 ml culture of *N. magadii* ΔORF35 or ΔORF36 were incubated at 37°C until complete lysis was achieved. After centrifugation for 10 min at 10 krpm, a drop of $CHCl_3$ was added to the supernatant. Afterwards, 100 µl of the supernatant were added to 500 µl of fresh *N. magadii* L13 culture with an OD_{600} 0.5-0.6. This was done in duplicates with the following dilutions: undiluted, 10^{-1} and 10^{-2}. The mixtures were incubated at 37°C for one hour without agitation to allow binding of the viruses to the L13 cells. Afterwards, they were washed twice with NVM+ medium and plated onto NVM+ Novobiocin plates. Single colonies were picked and tested via PCR for the desired construct.

Results and Discussion

Deletion of *int1* in *N. magadii* L11

Construction of the deletion mutant

In order to delete ORF35, located within the invertible region of ϕCh1 (nu. 24919-25593, accession number of ϕCh1: AF440695), the up- and down-stream sequences of ORF35 were amplified and cloned into pKS_{II}^{+}. Between these sequences, a novobiocin resistant cassette was introduced for selection of transformants. These sequences were amplified via PCR and cloned into pKS_{II}^{+} via Gibson assembly (Schülein, 2019). Positive clones were analyzed by sequencing and named ΔORF35.

The deletion plasmid ΔORF35 was transformed into *N. magadii* L11 to substitute ORF35 with a novobiocin resistance cassette. Single colonies were tested via PCR (data not shown). One of the positive clones was grown until lysed, centrifuged and the pellet was discarded. The supernatant was used to infect fresh *N. magadii* L13 cultures to ensure homogeneity in the deletion of *int1*. The cultures were plated again on selective media and incubated at 42°C.

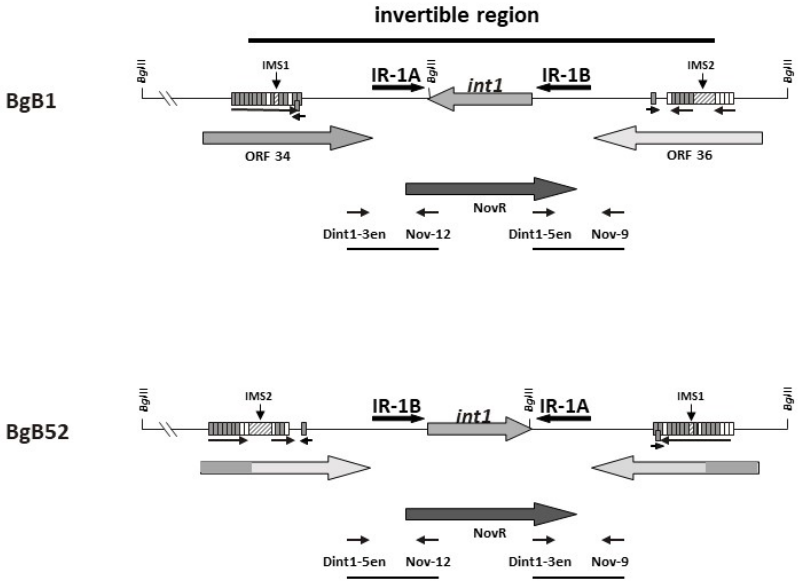

Figure 4: schematic graph of the invertible region of ϕCh1 showing two possible orientations (BgB1 and BgB52, respectively)The int1 *open reading frame is indicated as a large arrow, and the repeats found within the distinct clones are displayed as small boxes. Repeats containing the conserved 5´-end ATGGAcgC are indicated in grey, and repeats with mismatches within this sequence are marked with white boxes. Small black arrows indicate the orientation of the repeats. Overlapping, reversed repeats within a cluster are drawn staggered and slightly lower with respect to the others. Above clone Bgb1, the invertible region is marked with a line. Two other sequences within the repeat clusters are marked with white boxes containing inclined lines: the 207-bp-long intermediate sequence 2 (IMS2), which is identical in all clones independent of the different inverted repeats, as well as the 33-bp-long intermediate sequence 1 (IMS1), again identical in all clones. Diagonal slashes on the left indicate regions that are not indicated in the*

representation. Large arrows below the repeat clusters indicate the composition of ORF34 and ORF36 as well as their variants. Below each variant, the novobiocin cassette is indicated as an arrow. In addition the used primers and their location are indicated. The BglII *restriction sites are indicated (Rössler et al., 2004).*

Due to the possible integration of the suicide cassette into both possible variants of ϕCh1 (Rössler et al., 2004, see Fig. 4), first the 3´cross over was tested for both orientations. Therefore, after the re-adsorption into *N. magadii* L13, single colonies were tested for the 3' end (with respect to the orientation of ORF35 within the genome of ϕCh1) of the construct, using the primers Dint1-3en and Nov-12 (Fig. 5A).

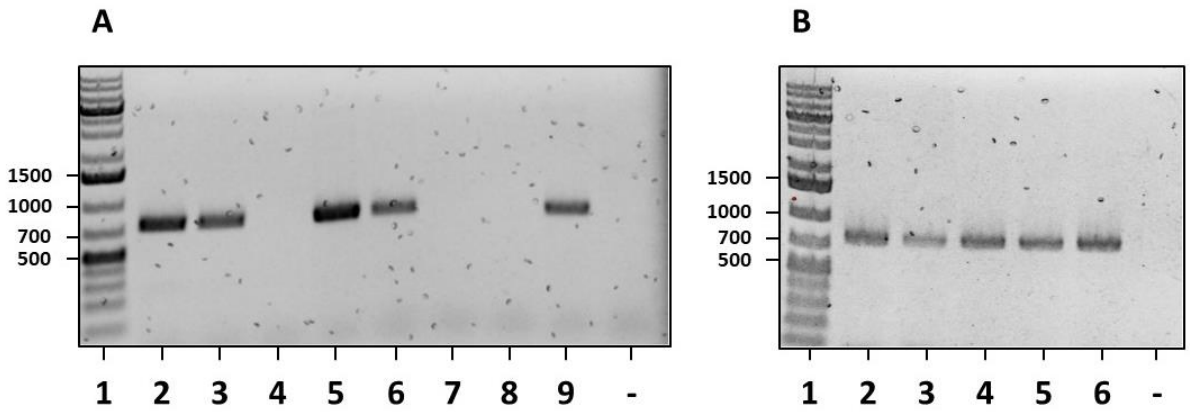

Figure 5: PCR test for 3' and 5´ cross over of N. magadii *L11-ΔORF35 construct. A: lane 1: GeneRuler 1 kb Plus DNA Ladder (only the relevant marker bands are indicated); lane 2 to 9: clones tested with primers Dint1-3en and Nov-12, lanes 2,3,5,6,9: clones positive for 3' end of ΔORF35 construct; lane 4, 7, 8: clones negative for 3' end of ΔORF35 construct; lane 10: negative control (template:* N. magadii *L11 wild type) B: lane 1: GeneRuler 1 kb Plus DNA Ladder (only the relevant marker bands are indicated); lane 2-6: positive 3' clones positive for 5' end of construct as well; lane 7: negative control (template:* N. magadii *L11 wild type)*

Five positive clones were obtained with the same orientation as in BgB1 as indicated in Figure 4 which were then tested for the 5' end of the construct in the $ORF34_1$ orientation with the primers Dint1-5en and Nov-9 (Fig. 5B).

Again, for all clones a specific PCR fragment was detected demonstrating that they were positive for the 5' end as well. As a last step, the colonies were tested for ORF35 for which no PCR product was expected to confirm its absence (Fig. 6).

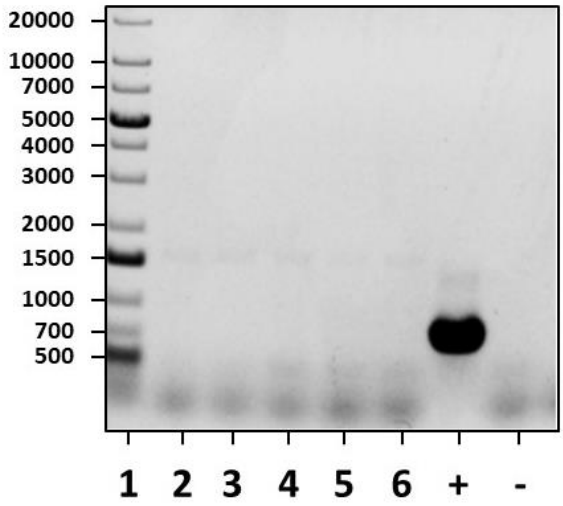

Figure 6: PCR deletion analysis of the presence of ORF35, lane 1: GeneRuler 1 kb Plus DNA Ladder; lane 2-6: clones positive for 3' and 5' end of ΔORF35; +: positive control (template N. magadii *L11); – : negative control (*N. magadii *L13).*

A specific PCR product was only obtained for the positive control (*N. magadii* L11) but neither for the 5 clones nor the negative control establishing the absence of *int1* in all five clones.

Southern Blot

To further confirm the deletion of *int1* in *N. magadii* L11, a Southern Blot was performed. DNA was extracted from the wild type and the deletion mutant to be restricted with the restriction enzyme *Pvu*II. The restricted DNA was then separated on an agarose gel, blotted and a Southern Blot performed (Fig. 8). The probes were designed to bind to both the wild type and the deletion mutant with the corresponding DNA fragments being of different sizes. Their positions are indicated in Fig. 7, marked with P1 and P2.

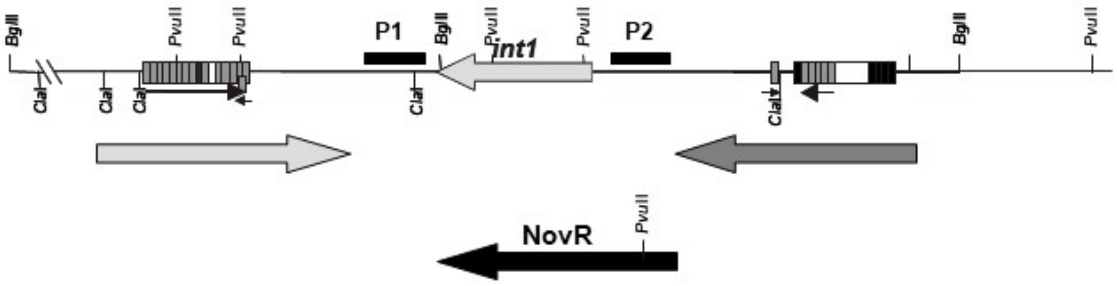

*Figure 7: Localization of the probes P1 and P2 used for Southern blot hybridization. The restriction sites of the region of ϕCh1, containing ORF35 (*int1*) are indicated as well as the probes used for Southern hybridization. The repeats as well as the open reading frames are the same as indicated in Fig. 4. Below the novobiocin resistance cassette of the mutant strain ϕCh1-Δ*int1 *is indicated.*

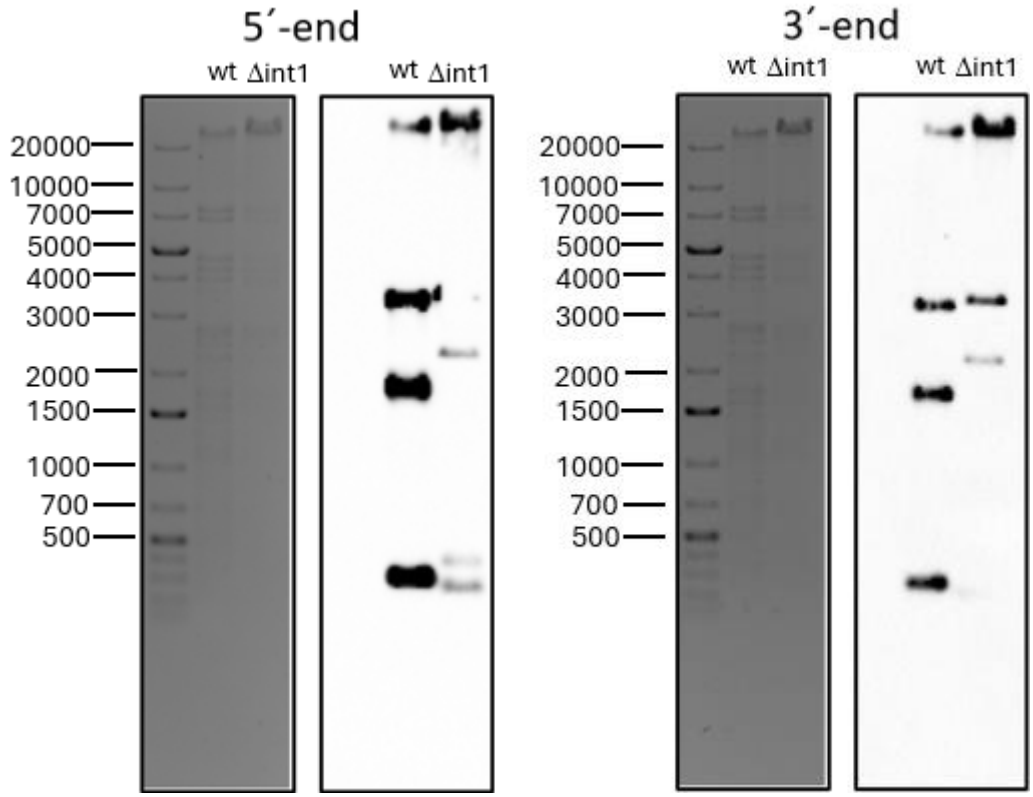

Figure 8: Southern Blot done with wild type N. magadii *L11 (wt) and* N. magadii *L11 ΔORF35 deletion mutant (Δ*int1*). Int1 is encoded by ORF35.*

Clear differences can be seen between the wild type and the deletion mutant for both the 5' and 3' end. The expected bands for the wild type have a length of 1700bp for the 5' end and 1215bp for the 3' end whereas the mutant bands are 2125bp long for the 5' and 2566bp for the 3'. Apart from the expected bands other bands can be seen probably due to partial restriction of the DNA.

However, a comparison between the 5´- and 3´- ends of both strains showed no differences as expected from the location of the used restriction endonuclease sites (see Fig. 7). This is due to the repeats between ORF34 and ORF35 as well as ORF35 and ORF36, called IR1-A and IR1-B (Fig. 4). An alignment of both sequences (see below) showed a stretch of 89 identical nucleotides, giving rise to the identical signals seen in the southern hybridization.

```
IR1-A     ATGCAACTGATCTTCACACCGGATGACTCCGGCACGAACCGGGCGAGTGGCTACGCGACC  60
          ||| |||| || |||||||||||| || |||||||||||| ||||||||||||||||||||
IR1-B     ATGGAACTCATTTTCACACCGGAGGATTCCGGCACGAAGCGGGCGAGTGGCTACGCGACC  225


IR1-A     GTTCCATACTCCAGTGACAGCGAA-GAGGAAACGGTCGCCGAAA  103
          |||||||||||||| ||  ||| | || || |||||||  ||||
IR1-B     GTTCCATACTCCAGCGAT-GCGGAGGACGAGACGGTCGTTGAAA  182
```

Score:108 bits(58), Expect:2e-28, Identities:89/104(86%), Gaps:2/104(1%), Strand: Plus/Minus

In order to verify these results, a second Southern Blot was performed with probes covering the 3´-ends of ORF34 and ORF36 to avoid an interaction with any repeat sequence (Fig. 9).

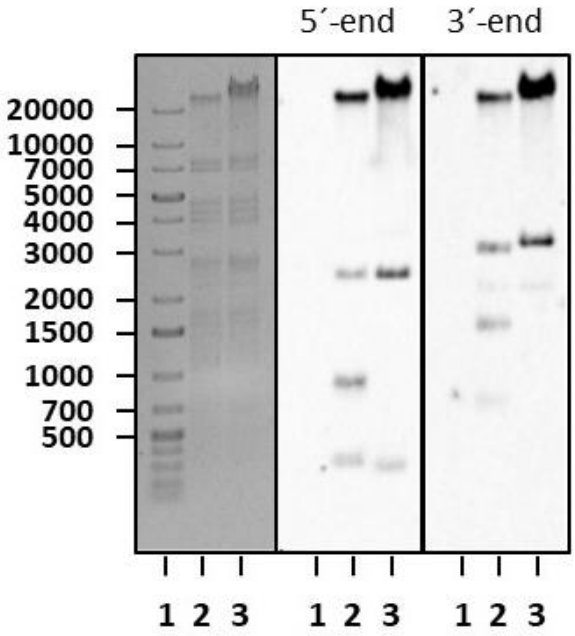

Figure 9: Southern Blot done with wild type N. magadii *L11 (wt) and* N. magadii *L11 ΔORF35 deletion mutant (Δ*int1*) as* int1 *is encoded by ORF35. The probe for the 5´-end was amplified with the primers 34-D-5/34-3, and the 3´-end with the primers 36-D-5/36-3.*

As can be seen in Figure 9, there are no common signals. It can therefore be assumed that the deletion strain no longer carries a copy of ORF35. The additional bands that are common are again due to partial digestion.

Growth Curve

Two clones were used to perform a growth curve for the duration of one week (Fig. 10) during which daily samples were taken at the same time points to use for the virus titer analysis and Western Blot.

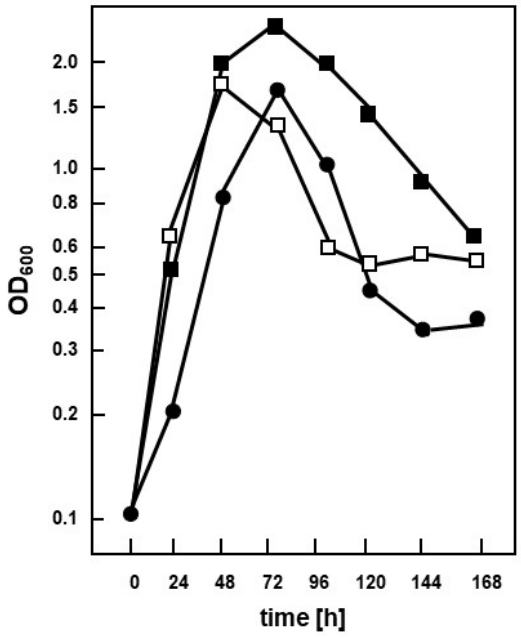

Figure 10: Growth curve of N. magadii *L11 and* N. magadii *L11 ΔORF35 clone 1 and 2.*
The optical density of all strains, grown at 37°C, was measured at 600 nm daily. Black circle: wild type N. magadii *L11, black square:* N. magadii *L11 ΔORF35 clone 1, white square:* N. magadii *L11 ΔORF35 clone 2. At the same time points samples were taken to measure the amount of infectious particles and for western blot analysis.*

Clone 1 and 2 showed different lysis behaviors as clone 2 already started to lyse after day 2 whereas the lysis of clone 1 began after day 4 and also seemed more prolonged than for clone 2. In this respect, clone 1 has a stronger resemblance to the wild type than clone 2.

Virus Titer Analysis

The virus titer was analyzed via plaque assay done in duplicates for both Δ*int1* mutants as well as the L11 wild type (Fig. 11).

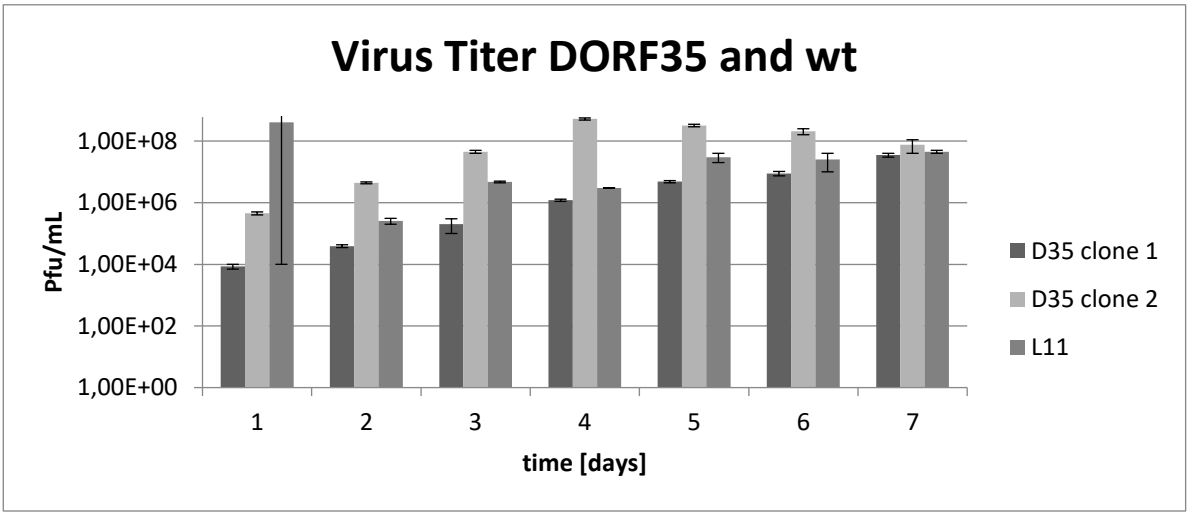

Figure 11: Determination of virus titer for int1 *deletion mutants and wild type L11 during the course of one week. Appropriate dilutions were prepared, mixed with the cured strain* N. magadii *L13 and poured onto a plate with top agar. The plates were incubated for at least 7 days at 37°C.*

The virus titer for the two different deletion mutants yielded remarkably different results. The titer of clone 1 is perceptively lower than the titer of the wild type which is expected as only the rearranged version $gp34_{52}$ was shown to bind to *N. magadii* (Klein et al., 2012). The titer of clone 2 on the other hand is noticeably higher than both the titer of clone 1 and the wild type.

How can this be? At any given time before the deletion of *int1*, both the recombined and not recombined form of ORF34 can be found in a population of ϕCh1. Therefore, it could happen that the deletion mutant contains either $ORF34_1$ or $ORF34_{52}$. For this reason, the PCR test for the 5' end of the construct was designed to be specific for $ORF34_1$. In a previous step of the experiment, both the PCR test for $ORF34_1$ and $ORF34_{52}$ led to a specific product. As one clone can only contain either $ORF34_1$ or $ORF34_{52}$, it suggests that when using this PCR reaction it might not be possible to distinguish between the two forms as it potentially introduces inversion reactions itself as seen for the experiment investigating the deletion of *int1* in a virus free background and in the literature (Hommelsheim et al., 2014; Meyerhans, 1990; Odelberg et al., 1995; Potapov & Ong, 2017).

This would explain the different results, as the deletion mutant containing $ORF34_1$ is expected to produce results similar to clone 1 with its reduced virus titer. Furthermore, the deletion mutant containing $ORF34_{52}$ could conceivably produce data akin to the ones of clone 2 as more of the binding $gp34_{52}$ should be produced.

Western Blot

To investigate if $gp34_{52}$ could still be detected in the *int1* deletion mutants throughout the time series, a Western Blot was performed using an antibody against $gp34_{52}$.

As a first step, the Western Blot samples which were taken daily during the growth curve were applied to an SDS gel and Coomassie stained to determine which volumes should be loaded for the respective samples. The following loading scheme was devised:

Clone 1		Clone 2		*N. magadii* L11	
Sample	**Amount [µl]**	**Sample**	**Amount [µl]**	**Sample**	**Amount [µl]**
1	12	1	12	1	10
2	12	2	12	2	10
3	10	3	10	3	10
4	11	4	11	4	10
5	10	5	10	5	10
6	10	6	10	6	10
7	11	7	11	7	10

A new SDS gel was loaded with the appropriate sample volumes. After the semi dry transfer and the first washing steps, the membrane was incubated with the primary antibody α-gp34$_{52}$ raised in rabbit. After three more washing steps, the incubation with the secondary anti-rabbit antibody and the final washing steps, chemiluminescence was used for detection (Fig. 12).

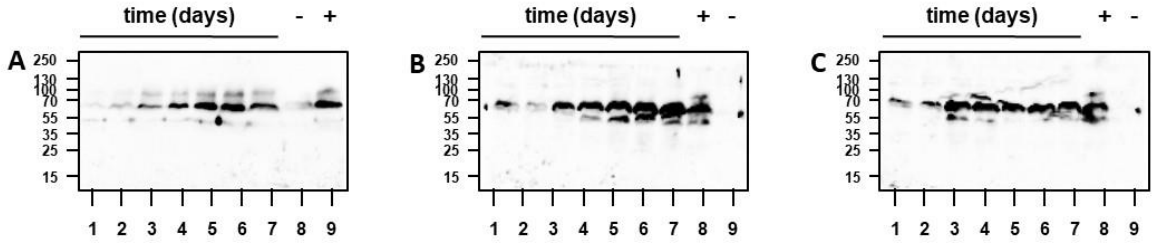

Figure 12: Western Blot with antibody against gp34$_{52}$ for time course of N.magadii *L11ΔORF35 clone 1 (B) and 2 (C).*
A: N.magadii *L11; marker: PageRuler™ Plus Prestained Protein Ladder, 10 bis 250 kDa; lane 1-7: sample from day 1-7; – : negative control (L13); +: positive control (L11)*
B: N.magadii *L11ΔORF35 clone 1; marker: PageRuler™ Plus Prestained Protein Ladder, 10 bis 250 kDa, lane 1-7: sample from day 1-7; +: positive control (L11); – : negative control (L13)*
C: N.magadii *L11ΔORF35 clone 2; marker: PageRuler™ Plus Prestained Protein Ladder, 10 bis 250 kDa, lane 1-7: sample from day 1-7; +: positive control (L11); – : negative control (L13)*

For the wild type *N. magadii* L11 a specific band was detected starting either very faintly on the first day or more visible on the second day throughout the whole time course. For both *int1* deletion mutants a specific product was detected throughout the course of the entire experiment. On the first two days, the band for gp34$_{52}$ was faint for both clones but a clear increase can be seen on the later days. This is surprising, as the antibody is specific for gp34$_{52}$. Since gp34$_{52}$ is produced by the inversion and consequent switch of the 3' ends of ORF34 and ORF36 mediated by *int1*, no bands should be visible as an *int1* deletion mutant was investigated.

For clone 2, this is not surprising as the clone is believed to contain ORF34$_{52}$ instead of ORF34$_{1}$ and therefore a signal is expected.

The bands for clone 1 can potentially be explained by the unspecificity of the primary antibody as it was shown to recognize both gp34 and gp36 due to their high sequence similarity mostly caused by nearly identical, repetitive stretches of aa residues (Klein et al., 2012; Rössler et al., 2004). Hence, it stands to reason that both the not recombined gp34$_{1}$ and the recombination product of ORF34 and ORF36 gp34$_{52}$ would be recognized by the same antibody as well as they too show a remarkable similarity in their sequence.

Conclusion

ORF35 of ϕCh1 is believed to code for an invertase (*int1*) inverting itself and the 3' end of its two neighboring ORFs, ORF34 and ORF36, which are generally in an inverted orientation towards each other (Klein et al., 2012; Ladurner, 2008; Rössler et al., 2004). To further investigate this, *int1* deletion mutants were produced via a deletion plasmid, exchanging *int1* with a novobiocin resistance cassette. Two clones were selected for the following experiments.

Two Southern Blots were performed to provide further evidence of the complete deletion of *int1* which indeed proved to be successful (Fig. 8 and 9). Additional bands are in all likelihood due to a partial DNA digestion by the restriction enzyme.

Next, a growth curve was done with both mutants and the wild type L11. Interestingly, clone 2 already started lysing a day before clone 1 and also seemed to lyse more rapidly as the lysis seemed to have only taken two days. For both clone 1 and the wily type the lysis set in after day 4 and was more prolonged (Fig. 10).

The plaque assay done with samples from the growth curve showed striking differences between the two clones as well (Fig. 11). Clone 1 produced the expected results with its virus titer being definitely lower than the wild type. Clone 2 on the other hand had a noticeably higher virus titer than the wild type. Considering the different lysis behaviors and the known inaccuracy of the *Taq* polymerase when amplifying repetitive or inverted sequences (Hommelsheim et al., 2014; Meyerhans, 1990; Odelberg et al., 1995; Potapov & Ong, 2017) seen as well for the investigation of the *int1* deletion in a virus free background, the explanation could be that the ORF34$_{1}$ specific PCR might not be specific enough and yields a product for ORF34$_{52}$ as well.

In a previous step, the clones were tested for both ORF34$_{1}$ and ORF34$_{52}$. Strikingly, for all clones a specific PCR product was obtained for ORF34$_{1}$ and ORF34$_{52}$ which should not be the case. This can easily be explained if through the PCR reaction itself an inversion would be introduced. Therefore,

clone 2 could in reality contain ORF34$_{52}$ whereas clone 1 truly does contain ORF34$_1$. This would firstly explain the different results and secondly reinforce the hypothesis that *int1* is involved in the inversion reaction as the two clones would have otherwise produced more similar results as an inversion reaction would have happened. Thirdly, this is in accordance with previous results showing the binding of gp34$_{52}$ to *N. magadii* in comparison to gp34$_1$ (Klein et al., 2012) as the virus titer of the presumed clone containing ORF34$_{52}$ was strikingly higher than of the wild type.

The Western Blot done with the growth curve samples showed a specific band for both deletion mutants and the wild type when detected with an antibody raised against gp34$_{52}$ (Fig. 12). As no inversion should occur and both mutants were believed to only contain ORF34$_1$ these results were unexpected.

For clone 2 these signals can be easily explained, as it is thought to contain ORF34$_{52}$ instead of ORF34$_1$. On the other hand, the bands of clone 1 are probably detected due to the unspecificity of the antibody as it was shown in previous experiments to be incapable of distinguishing between gp34 and gp36 due to their nearly identical, repetitive stretches of aa residues (Klein et al., 2002; Klein et al., 20212; Rössler et al., 2004). Therefore, this antibody binds in all likelihood to both gp34$_{52}$ and gp34$_1$. For this reason, no conclusion can be drawn whether the detected proteins arose to inversion or not.

Taken together, these experiments could provide further evidence for the inversion reaction of ORF34 and ORF36 mediated by *int1* if the correct genotypes could be determined. Therefore, future experiments could either focus on developing a different setup for the problematic PCR reactions or finding a way to circumvent the PCR reactions all together.

Investigation of *int1* deletion in virus free background

The construct pRo-5 52-2 containing ORF 34_{52}, ORF35 and $ORF36_{52}$ and the construct pRo-5 52-3 containing ORF 34_{52} and 36_{52} (Fig. 13) were cloned into *N. magadii* L13 to investigate the effect of the missing ORF35 on the inversion reaction. The non-rearranged fragment was amplified with the primers 34-5 and 36-3 whereas the inverted fragment was amplified using the primers 34-5 and 34-3.

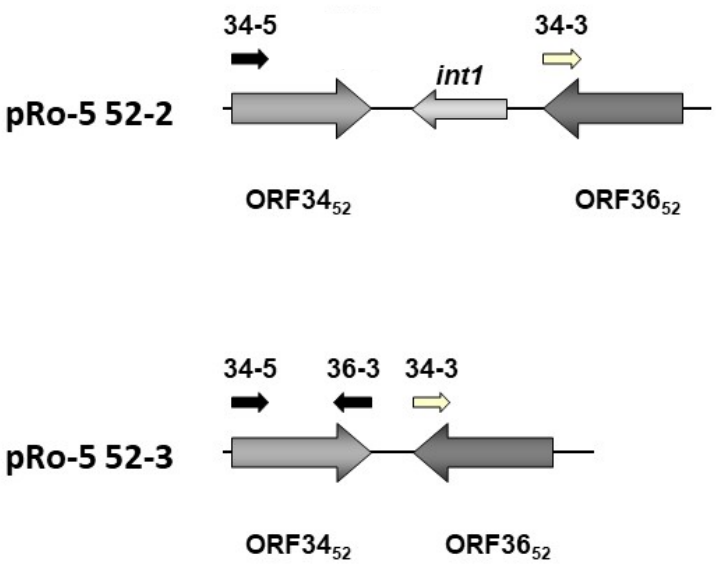

Figure 13: plasmids pRo-5 52-2 and pRo-5 52-3, including the respective primers used in the following analyses, adapted from Ladurner, 2008

Testing different Polymerases

*2x*GoTaq *Green Master Mix*

The 2x*GoTaq* Green Master Mix was used to test for inversion reactions during a 7 day long growth period of *N. magadii* L13 containing either plasmid pRo-5 52-2 or pRo-5 52-3 (Fig. 14).

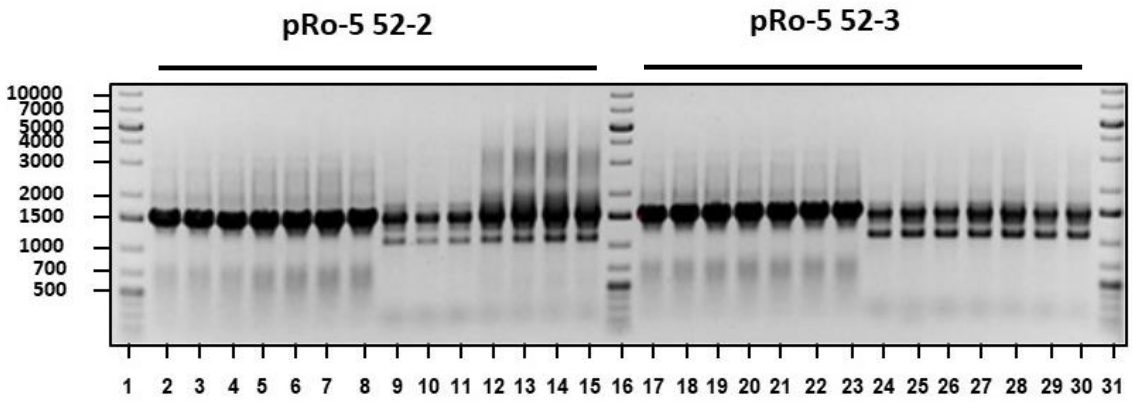

Figure 44: Daily samples were taken of N.magadii *L13 (pRo5- 52 2) and* N.magadii *L13 (pRo-5 52-3) for one week and tested for inverted and not inverted fragments of ORF34 and ORF36. Lane 1, 16, 31: GeneRuler 1 kb Plus DNA Ladder; lane 2-8: L13 (pRo5-52-2) day 1-7, tested for not inverted fragment; lane 9-15: L13 (pRo5-52-2) day 1-7, tested for inverted fragment; lane 17-23: L13 (pRo5-52-3) day 1-7, tested for not inverted fragment; lane 24-30: L13 (pRo5-52-3) day 1-7, tested for inverted fragment*

For both constructs PCR products were detected when testing for the inverted fragments as well as the non-rearranged fragments. This is in stark contrast to previous results where inversion reactions were detected solely for L13 (pRo-5 52-2) and this only beginning on the third day of the growth curve (Fig. 15; Ladurner, 2008). The same holds true for a growth curve done with L11 for which the inversion reaction was traceable from the third day onwards (Klein et al., 2012).

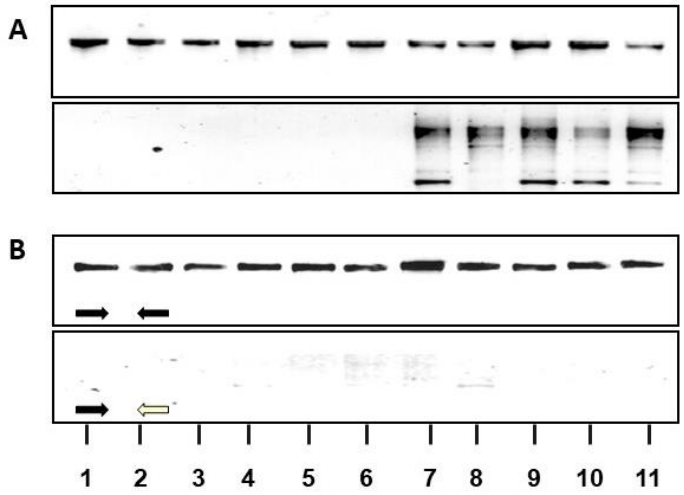

Figure 15: Analysis of int1 *in* N. mag. *L13 using the plasmids pRo-5 52-2 and pRo-5 52-3.*
1-11 indicate the sample time points 0h, 7.5h, 22.5h, 30.5h, 54.25h, 71h, 78h, 102.25h, 120.75h, 144.75h and 167.25h after inoculation.
A) L13 (pRo-5 52-2), the upper panel shows the PCR products obtained from test for the not inverted fragment (primers 34-5 and 36-3) whereas the lower panel shows the PCR reactions done for the inverted fragment (primers 34-5 and 34-3).
B) L13 (pRo-5 52-3), the upper panel shows the PCR products obtained from test for the not inverted fragment (primers 34-5 and 36-3, black left and black right arrow) whereas the lower panel shows the PCR reactions done for the inverted fragment (primers 34-5 and 34-3, black left and light right arrow) (adapted from Ladurner, 2008).

As no inverted fragments should be detected in L13 (pRo-5 52-3) and the inversion reaction was shown to occur later in the growth phase for both the wild type and L13 (pRo-5 52-2), the differences between the previous and current experiments were analyzed.

The polymerase was found to be the main difference as the original polymerase could not be purchased any longer. It has long been known that the *Taq* polymerase can recombine DNA molecules by itself especially homologous, repetitive or inverted sequences (Hommelsheim et al., 2014; Meyerhans, 1990; Odelberg et al., 1995) which can be found in this construct plentifully. In a recent study, Potapov and Ong investigated this phenomenon using other polymerases as well. Most polymerases were found to introduce inversion reactions by themselves. Notably, the

polymerase introducing the least inversions was the exonuclease-deficient variant of *Deep Vent (exo-)* polymerase suggesting that abolishing proofreading activity may increase the ability of the polymerase to accurately replicate without introducing large scale inversions (Potapov & Ong, 2017).

Therefore, other polymerases were tested using the daily growth curve samples of L13 (pRo-5 52-2) and L13 (pRo-5 52-3).

Phusion *High Fidelity Master Mix*

Again, the growth curve samples of L13 (pRo-5 52-2) and L13 (pRo-5 52-3) were tested via PCR using the primer pairs 34-5/36-3 and 34-5/34-3 together with the *Phusion* High Fidelity Master Mix. Both the wild type and the mutant PCRs produced an inversion specific construct (Fig. 16). For both L13 (pRo-5 52-2) and L13 (pRo-5 52-3) no inversion specific product was obtained for day 1. In addition, for L13 (pRo-5 52-3) no PCR product was obtained for day 1 not inverted and for day 6 inverted. This is due to a technical mistake.

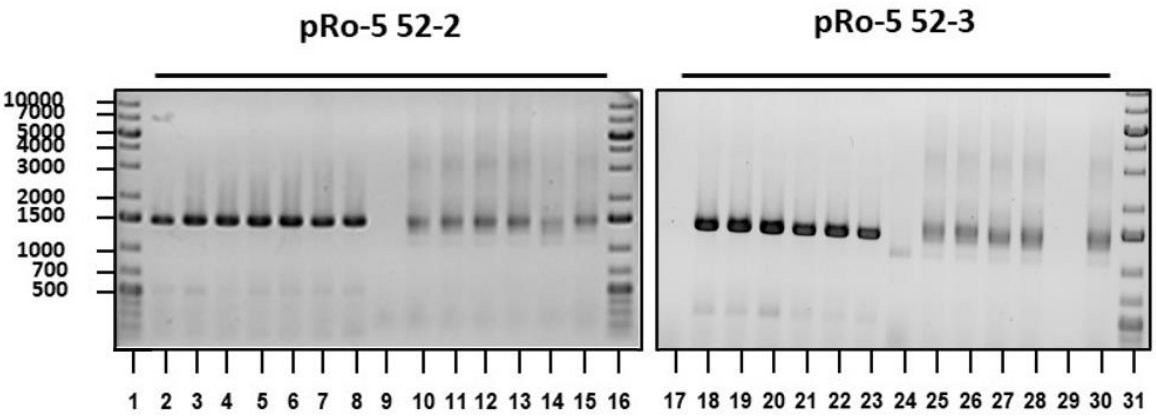

Figure 16: Daily samples were taken of L13 (pRo5- 52 2) and L13 (pRo-5 52-3) for one week and tested for inverted and not inverted fragments of ORF34 and ORF36. Lane 1, 16, 31: GeneRuler 1 kb Plus DNA Ladder; lane 2-8: L13 (pRo5-52-2) day 1-7, tested for not inverted fragment; lane 9-15: L13 (pRo5-52-2) day 1-7, tested for inverted fragment; lane 17-23: L13 (pRo5-52-3) day 1-7, tested for not inverted fragment; lane 24-30: L13 (pRo5-52-3) day 1-7, tested for inverted fragment

Pwo *polymerase*

Next, the *Pwo* polymerase was used to analyze the growth curve samples of L13 (pRo-5 52-2) and L13 (pRo-5 52-3).

The results were again similar to the PCR products obtained by other polymerases (Fig.17). A specific PCR product was obtained for both constructs at almost all time points, except for the inversion reactions for both constructs on day 1, again due to a technical error.

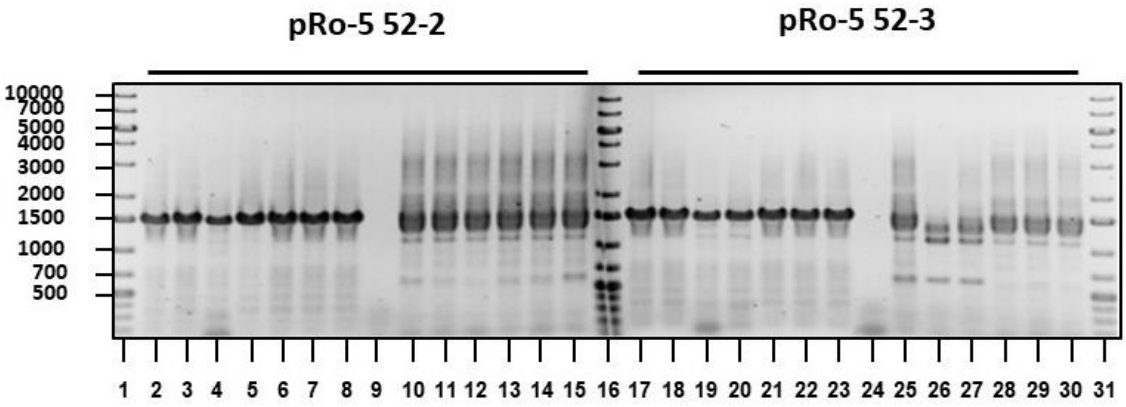

Figure 17: Daily samples were taken of L13 (pRo5- 52 2) and L13 (pRo-5 52-3) for one week and tested for inverted and not inverted fragments of ORF34 and ORF36. Lane 1, 16, 31: GeneRuler 1 kb Plus DNA Ladder; lane 2-8: L13 (pRo5-52-2) day 1-7, tested for not inverted fragment; lane 9-15: L13 (pRo5-52-2) day 1-7, tested for inverted fragment; lane 17-23: L13 (pRo5-52-3) day 1-7, tested for not inverted fragment; lane 24-30: L13 (pRo5-52-3) day 1-7, tested for inverted fragment

Pfu *polymerase*

The growth curve samples of L13 (pRo-5 52-2) and L13 (pRo-5 52-3) were tested with the *Pfu* polymerase as well and the results were akin to the results of the previously tested polymerases (Fig. 18). The primers 34-5 and 36-3 were used to test for the not inverted fragment and a specific band was obtain for every day for both constructs. The inverted fragments were tested for with the primer pair 34-5 and 34-3 and specific fragments were detected for all samples again no matter the construct or day.

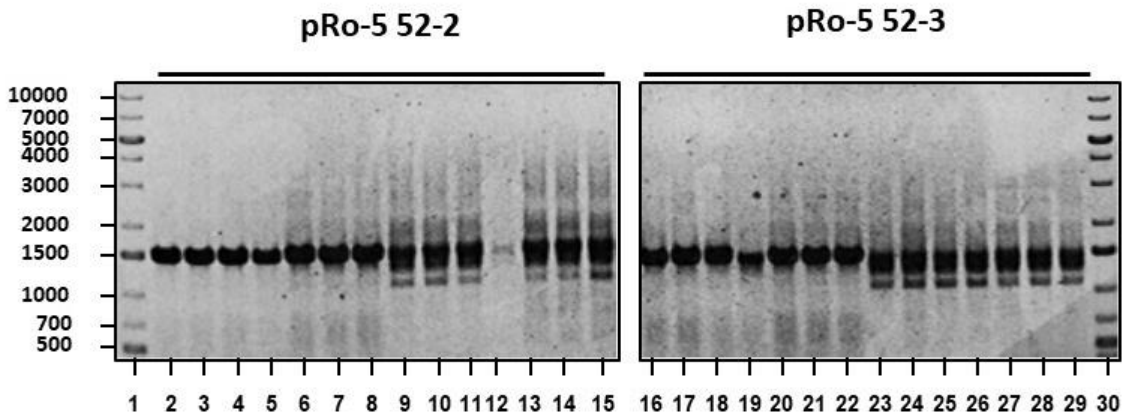

Figure 18: Daily samples were taken of L13 (pRo5- 52 2) and L13 (pRo-5 52-3) for one week and tested for inverted and not inverted fragments of ORF34 and ORF36. Lane 1, 30: GeneRuler 1 kb Plus DNA Ladder; lane 2-8: L13 (pRo5-52-2) day 1-7, tested for not inverted fragment; lane 9-15: L13 (pRo5-52-2) day 1-7, tested for inverted fragment; lane 16-22: L13 (pRo5-52-3) day 1-7, tested for not inverted fragment; lane 23-29: L13 (pRo5-52-3) day 1-7, tested for inverted fragment

Vent (exo-) *polymerase*

Preliminary tests were performed using the *vent (exo-)* polymerase but the results were unpromising therefore further experiments were discontinued (data not shown).

Conclusion

As polymerases are known to potentially yield unreliable results when amplifying repetitive sequences (Hommelsheim et al., 2014; Meyerhans, 1990; Odelberg et al., 1995; Potapov & Ong, 2017) and all tested polymerases yielded results in stark contrast to previous experiments, no suitable polymerase was found for this experimental setup. Therefore, no conclusions can be drawn in regards to the suspected inversion reactions or lack thereof in L13 (pRo-5 52-2) and L13 (pRo-5 52-3).

In future experiments, either more polymerases will have to be tested until a fitting one is found or a different experimental approach has to be chosen.

Construction of the deletion mutant *N. magadii* L11 ΔORF36$_{52}$

In order to further verify the function of different parts of the invertible region, the second open reading frame encoding possible tail fiber proteins should be deleted (Rössler et al., 2004).

Here, the deletion of ORF36 was started. As shown previously, ORF 34 and 36 exist in two different variations within the cell of *N. magadii* (Fig. 4). However, only one version is able to produce possible tail fibers for the successful infection of *N. magdii* L13: these proteins are encoded by the (-) segment (Klein et al., 2012).

Therefore, a deletion plasmid was constructed which should be able to integrate into the genomic DNA of ϕCh1. The upstream sequence for the recombination was amplified with primers DORF36-1 and DORF36-5R and the downstream sequence with primers DORF36-6R and DORF36-7R. Together with the novobiocin resistance cassette NovR (amplified with primers NovR-1p and NovR-2s) all fragments were introduced into the plasmid pKS$_{II}^{+}$ using Gibson assembly. The localization of the primes used for screening as well as the expected fragment length are indicated in Fig. 19 A. As shown in Fig. 19, 5 of 8 clones were positively screened for the upstream sequence and the NovR fragment (Fig. 19 B, left panel). These five clones were tested for the downstream sequence (Fig. 19 B, right panel). After sequencing of the clones, one was chosen and its deletion plasmid transformed into *N. magadii* L11. Again, eight transformants were inoculated and analyzed for the correct recombination event (Fig. 20 C).

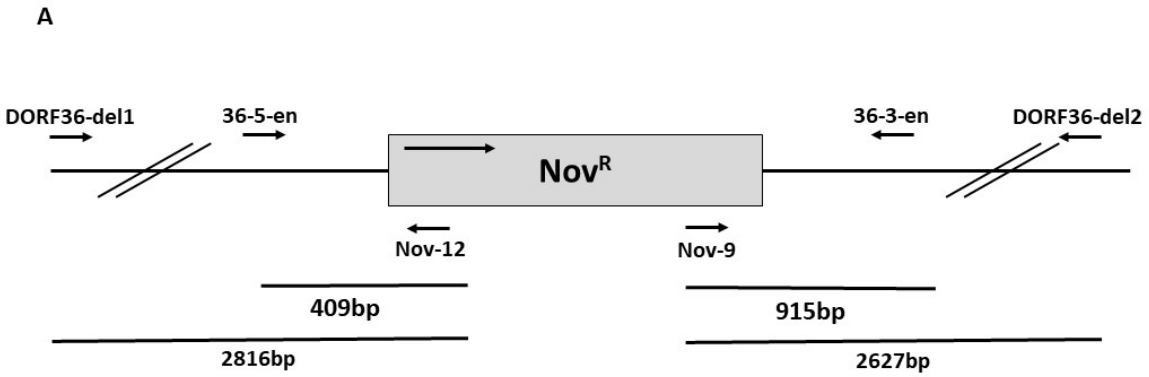

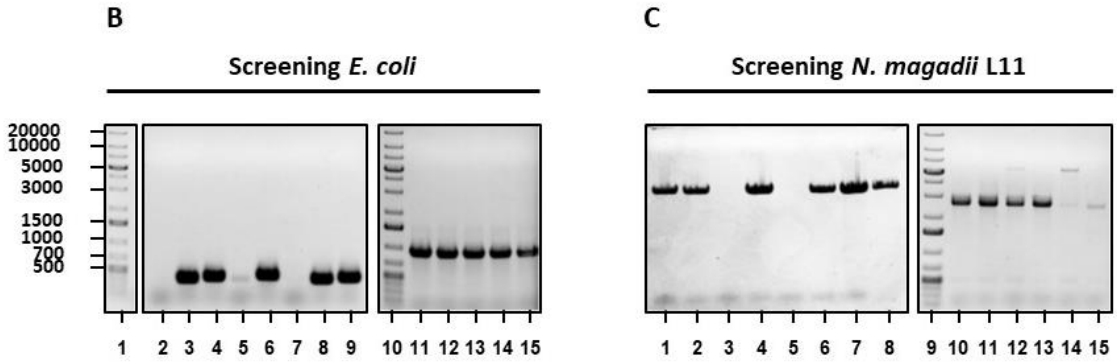

Figure 19: Construction of the deletion plasmid ΔORF36 and screening for recombinants in N. magadii *L11.*
A: Schematic graph of the novobiocin cassette as well as the primers and their localizations used for screening. The expected fragment lengths of the different products are indicated below the lines.
B: lanes 1 and 10: GeneRuler 1 kb Plus DNA Ladder; lane 2 to 9: clones tested with primers 36-en-5 and Nov-12, lanes 10 to 15: clones tested with primers 36-en-3 and Nov-9.
C: lane 9: GeneRuler 1 kb Plus DNA; lane 1 to 8: clones tested with primers DORF36-del1 and Nov-12; lane 10 to 15: clones tested with primers DORF36-del2 and Nov-9

Out of these four positive clones, one was inoculated again and the culture was grown until lysis was completed. The supernatant was used to re-infect *N. magadii* L13 to homogenize the deletion mutant ϕCh1 ΔORF36. After growth of inoculated transfectants, cultures were tested for a clone without ORF36. Therefore, primers DORF36-del1 and DORF36-del2 were used, binding outside of the region of the deleted ORF36 giving rise to a fragment with a length of 7715bp. This analysis would directly show both the deletion of ORF36 and the homogenization of the culture as well. However, as can be seen in Fig. 20 none of the cultures tested so far have contained the right fragment. Therefore, more clones have to be tested to find the correct construct.

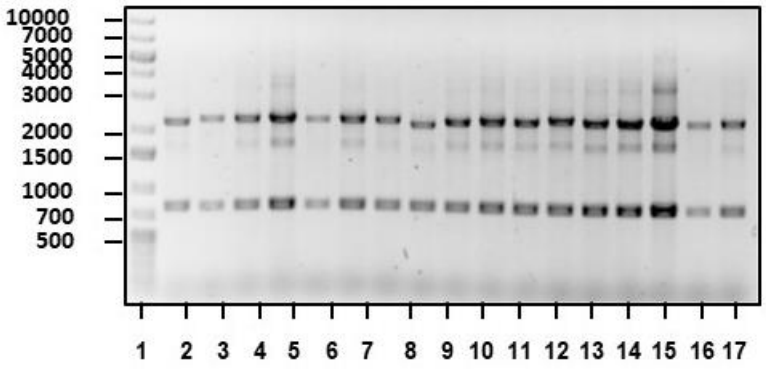

Figure 20: Screening for recombinants in N. magadii *L11 after re-infection.*
Lane 1: GeneRuler 1 kb Plus DNA Ladder; lane 2 to 17: different clones tested with primers DORF36-del1 and DORF36-del2

Conclusion

The construction of a deletion plasmid for ϕCh1 ORF36 via Gibson Assembly was successful but until now none of the tested clones contained the correct fragment. Though, as more clones are being tested a positive colony should be identified soon.

Overall Conclusion

The aim of this thesis was the analysis of the invertible region of ϕCh1. Here, two open reading frames are encoded, with the products encoding putative tail fiber proteins (Klein et al., 2012). The complete region undergoes a recombination event giving rise to a variety of different clones. One of the questions was to determine if ORF35, encoding a putative recombinase, is responsible for this event. The existence of numerous repeats in the open reading frames 34 and 36 indicate that these are used for recombination. After the successful construction of a deletion mutant, analyses were performed to answer this question. However, the used method was not successful. Most probably, this is due to the polymerases used in the PCRs of this studies. As shown previously, polymerases such as the *Taq* polymerase and others introduce substitutions and recombinations with different rates (Hommelsheim et al., 2014; Meyerhans, 1990; Odelberg et al., 1995; Potapov & Ong, 2017).

The analysis of -*int1* in a virus free background was unsuccessful as well in all likelihood due to the same reasons.

Furthermore, a deletion plasmid of ORF36 was successfully constructed, though no positive clone has been identified so far.

Therefore, the influence of Int1 and its neighboring repeat clusters on the inversion of the central region of ϕCh1 still remains enigmatic but hopefully the results of this study will nevertheless be of help in future experiments trying to unravel the many unsolved mysteries of ϕCh1.

Zusammenfassung

Der gemäßigte Kopf-Schwanz-Virus ϕCh1 beherbergt sich wiederholende Cluster (ORF34, ORF36) und eine Invertase (*int1*) in der zentralen Region seines Genoms. Die Inversion der 3'-Enden von ORF34 und ORF36 führt zur Expression eines rekombinanten Proteins $gp34_{52}$, das wiederum an der Infektion von *N. magadii* beteiligt ist, seinem einzig bekannten Wirt.

Zur weiteren Untersuchung dieser Inversion wurden zwei verschiedene Plasmide in *N. magadii* L13 geklont, einen von dem Virus geheilten Stamm, die entweder ORF34, *int1* und ORF36 oder nur ORF34 und ORF36 enthielten. Die Proben der Wachstumskurven wurden mittels PCR analysiert. Da Polymerasen bei der Amplifikation von repetitiven Sequenzen bekanntermaßen unzuverlässig sind und die Ergebnisse stark von früheren Ergebnissen abwichen, die mit einer inzwischen nicht mehr verfügbaren Polymerase erzielt wurden, konnte keine konkrete Schlussfolgerung gezogen werden.

Zusätzlich wurden *int1*-Deletionsmutanten durch Deletionsplasmide hergestellt. Die Deletion wurde mittels PCR und Southern Blot bestätigt, gefolgt von Plaque-Assays und Western Blots. Die beiden untersuchten Mutanten wiesen unterschiedliche Infektiositäten auf, da ein Klon vermutlich ORF34 in seiner nicht rekombinierten Form und der andere in seiner rekombinierten Form trägt. Aufgrund von PCR-Ungenauigkeiten war es nicht möglich, die Klone zweifelsfrei zu klassifizieren. Die Western Blots der beiden zeigten ein Signal für das rekombinante $gp34_{52}$, aber der verwendete Antikörper konnte bisher nicht zwischen gp34 und gp36 unterscheiden. Daher sind weitere Untersuchungen notwendig.

Außerdem wurde ein Deletionsplasmid von ORF36 in umgekehrter Orientierung konstruiert, um eine ΔORF36 Mutante zu erzeugen. Bislang konnte aber noch kein positiver Klon identifiziert werden.

References

Altermann, E., Schofield, L. R., Ronimus, R. S., Beatty, A. K., & Reilly, K. (2018). Inhibition of Rumen methanogens by a novel archaeal lytic enzyme displayed on tailored bionanoparticles. *Frontiers in Microbiology*, *9*(OCT). https://doi.org/10.3389/fmicb.2018.02378

Baker, B. J., De Anda, V., Seitz, K. W., Dombrowski, N., Santoro, A. E., & Lloyd, K. G. (2020). Diversity, ecology and evolution of Archaea. In *Nature Microbiology* (Vol. 5, Issue 7, pp. 887–900). Nature Research. https://doi.org/10.1038/s41564-020-0715-z

Baquero, D. P., Liu, J., & Prangishvili, D. (2021). Egress of archaeal viruses. In *Cellular Microbiology* (Vol. 23, Issue 12). John Wiley and Sons Inc. https://doi.org/10.1111/cmi.13394

Bettstetter, M., Peng, X., Garrett, R. A., & Prangishvili, D. (2003). AFV1, a novel virus infecting hyperthermophilic archaea of the genus Acidianus. *Virology*, *315*(1), 68–79. https://doi.org/10.1016/S0042-6822(03)00481-1

Bize, A., Karlsson, E. A., Ekefjä Rd B, K., Quax, T. E. F., Pina, M., Prevost, M.-C., Forterre, P., Tenaillon, O., Bernander, R., & Prangishvili, D. (2009). *A unique virus release mechanism in the Archaea*. www.pnas.orgcgidoi10.1073pnas.0901238106

Breuert, S., Allers, T., Spohn, G., & Soppa, J. (2006). Regulated polyploidy in halophilic archaea. *PLoS ONE*, *1*(1). https://doi.org/10.1371/journal.pone.0000092

Brumfield, S. K., Ortmann, A. C., Ruigrok, V., Suci, P., Douglas, T., & Young, M. J. (2009). Particle Assembly and Ultrastructural Features Associated with Replication of the Lytic Archaeal Virus Sulfolobus Turreted Icosahedral Virus . *Journal of Virology*, *83*(12), 5964–5970. https://doi.org/10.1128/jvi.02668-08

Brüssow, H., & Desiere, F. (2001). Comparative phage genomics and the evolution of siphoviridae: Insights from dairy phages. In *Molecular Microbiology* (Vol. 39, Issue 2, pp. 213–223). Blackwell Publishing Ltd. https://doi.org/10.1046/j.1365-2958.2001.02228.x

Daum, B., Quax, T. E. F., Sachse, M., Mills, D. J., Reimann, J., Yildiz, Ö., Häder, S., Saveanu, C., Forterre, P., Albers, S. V., Kühlbrandt, W., & Prangishvili, D. (2014). Self-assembly of the general membrane-remodeling protein PVAP into sevenfold virus-associated pyramids. *Proceedings of the National Academy of Sciences of the United States of America*, *111*(10), 3829–3834. https://doi.org/10.1073/pnas.1319245111

Demaere, M. Z., Williams, T. J., Allen, M. A., Brown, M. V., Gibson, J. A. E., Rich, J., Lauro, F. M., Dyall-Smith, M., Davenport, K. W., Woyke, T., Kyrpides, N. C., Tringe, S. G., & Cavicchioli, R. (2013). High level of intergenera gene exchange shapes the evolution of haloarchaea in an isolated Antarctic lake. *Proceedings of the National Academy of Sciences of the United States of America*, *110*(42), 16939–16944. https://doi.org/10.1073/pnas.1307090110

Dyall-Smith, M., Tang, S. L., & Bath, C. (2003). Haloarchaeal viruses: How diverse are they? In *Research in Microbiology* (Vol. 154, Issue 4, pp. 309–313). Elsevier Masson SAS. https://doi.org/10.1016/S0923-2508(03)00076-7

Falb, M., Müller, K., Königsmaier, L., Oberwinkler, T., Horn, P., Von Gronau, S., Gonzalez, O., Pfeiffer, F., Bornberg-Bauer, E., & Oesterhelt, D. (2008). Metabolism of halophilic archaea. In *Extremophiles* (Vol. 12, Issue 2, pp. 177–196). https://doi.org/10.1007/s00792-008-0138-x

Fendrihan, S., Legat, A., Pfaffenhuemer, M., Gruber, C., Weidler, G., Gerbl, F., & Stan-Lotter, H. (2006). Extremely halophilic archaea and the issue of long-term microbial survival. In *Reviews in Environmental Science and Biotechnology* (Vol. 5, Issues 2–3, pp. 203–218). https://doi.org/10.1007/s11157-006-0007-y

Forterre, P. (2013). The common ancestor of archaea and eukarya was not an archaeon. In *Archaea* (Vol. 2013). https://doi.org/10.1155/2013/372396

Hommelsheim, C., Frantzeskakis, L., Huang, M., Ülker, B. (2014). PCR amplification of repetitive DNA: A limitation to genome editing technologies and many other applications. In *Scientific Reports* (Vol. 4). https://doi.org/10.1038/srep05052

Hulbert, A. J., & Else, P. L. (2005). Membranes and the setting of energy demand. In *Journal of Experimental Biology* (Vol. 208, Issue 9, pp. 1593–1599). https://doi.org/10.1242/jeb.01482

Judo, M., Wedel, A., Wilson, C. (1998). Stimulation and suppression of PCR-mediated recombination. *Nucleic Acid Research* (Vol. 26, No. 7, pp. 1819-1825). https://academic.oup.com/nar/article/26/7/1819/1044437

Klein, R., Baranyi, U., Rössler, N., Greineder, B., Scholz, H., & Witte, A. (2002). Natrialba magadii virus ϕCh1: First complete nucleotide sequence and functional organization of a virus infecting a haloalkaliphilic archaeon. *Molecular Microbiology*, *45*(3), 851–863. https://doi.org/10.1046/j.1365-2958.2002.03064.x

Klein, R., Rössler, N., Iro, M., Scholz, H., & Witte, A. (2012). Haloarchaeal myovirus ϕCh1 harbours a phase variation system for the production of protein variants with distinct cell surface adhesion specificities. *Molecular Microbiology*, *83*(1), 137–150. https://doi.org/10.1111/j.1365-2958.2011.07921.x

Kok, J., Visweswaran, G. R. R., & Dijkstra, B. W. (2010). Two major archaeal pseudomurein endoisopeptidases: PeiW and PeiP. In *Archaea* (Vol. 2010). https://doi.org/10.1155/2010/480492

Krupovic, M., Cvirkaite-Krupovic, V., Iranzo, J., Prangishvili, D., & Koonin, E. V. (2018). Viruses of archaea: Structural, functional, environmental and evolutionary genomics. In *Virus Research* (Vol. 244, pp. 181–193). Elsevier B.V. https://doi.org/10.1016/j.virusres.2017.11.025

Ladurner, A. (2008). Characterization of the inversion reaction of ϕ Ch1 and the establishment of a transformation system for Natrialba magadii. *Diplomarbeit*.

Liu, J., Gao, R., Li, C., Ni, J., Yang, Z., Zhang, Q., Chen, H., & Shen, Y. (2017). Functional assignment of multiple ESCRT-III homologs in cell division and budding in Sulfolobus islandicus. *Molecular Microbiology*, *105*(4), 540–553. https://doi.org/10.1111/mmi.13716

Luk, A. W. S., Williams, T. J., Erdmann, S., Thane Papke, R., & Cavicchioli, R. (2014). Viruses of haloarchaea. In *Life* (Vol. 4, Issue 4, pp. 681–715). MDPI AG. https://doi.org/10.3390/life4040681

Macalady, J. L., Vestling, M. M., Baumler, D., Boekelheide, N., Kaspar, C. W., & Banfield, J. F. (2004). Tetraether-linked membrane monolayers in Ferroplasma spp: A key to survival in acid. *Extremophiles*, *8*(5), 411–419. https://doi.org/10.1007/s00792-004-0404-5

Mathai, J. C., Sprott, G. D., & Zeidel, M. L. (2001). Molecular Mechanisms of Water and Solute Transport across Archaebacterial Lipid Membranes. *Journal of Biological Chemistry*, *276*(29), 27266–27271. https://doi.org/10.1074/jbc.M103265200

Mayrhofer-Iro, M., Ladurner, A., Meissner, C., Derntl, C., Reiter, M., Haider, F., Dimmel, K., Rössler, N., Klein, R., Baranyi, U., Scholz, H., & Wittea, A. (2013). Utilization of virus ϕCh1 elements to establish a shuttle vector system for halo(alkali)philic Archaea via transformation of Natrialba magadii. *Applied and Environmental Microbiology*, *79*(8), 2741–2748. https://doi.org/10.1128/AEM.03287-12

Meyerhans, A., Vartanian, J., Wain-Hobson, S. (1990). DNA recombination during PCR. *Nucleic Acid Research* (Vol. 18, No. 7, pp. 1687-1691).

Munson-Mcgee, J. H., Snyder, J. C., & Young, M. J. (2018). Archaeal viruses from high-temperature environments. *Genes*, *9*(3). https://doi.org/10.3390/genes9030128

Odelberg, S., Weiss, R., Hata, A., White, R. (1995). Template-switching during DNA synthesis by *Thermus aquaticus* DNA polymerase I. *Nucleic Acid Research* (Vol. 23, No. 11, pp. 2049-2057).

Oren, A. (1994). The ecology of the extremely halophilic archaea. *FEMS Microbiology Reviews*, *13*(4), 415–439. https://doi.org/10.1111/j.1574-6976.1994.tb00060.x

Oren, A. (2002). Diversity of halophilic microorganisms: Environments, phylogeny, physiology, and applications. *Journal of Industrial Microbiology and Biotechnology*, *28*(1), 56–63. https://doi.org/10.1038/sj/jim/7000176

Pietilä, M. K., Demina, T. A., Atanasova, N. S., Oksanen, H. M., & Bamford, D. H. (2014). Archaeal viruses and bacteriophages: Comparisons and contrasts. *Trends in Microbiology*, *22*(6), 334–344. https://doi.org/10.1016/j.tim.2014.02.007

Potapov, V., Ong, J. (2017). Examining sources of error in PCR by single-molecule sequencing. *PLoS ONE* (Vol. 12, Issue 1). https://doi.org/10.1371/journal.pone.0169774

Prangishvili, D., Arnold, H. P., Götz, D., Ziese, U., Holz, I., Kristjansson, J. K., & Zillig, W. (1999). A Novel Virus Family, the Rudiviridae: Structure, Virus-Host Interactions and Genome Variability of the Sulfolobus Viruses SIRV1 and SIRV2. https://academic.oup.com/genetics/article/152/4/1387/6047759

Prangishvili, D., Bamford, D. H., Forterre, P., Iranzo, J., Koonin, E. V., & Krupovic, M. (2017). The enigmatic archaeal virosphere. In *Nature Reviews Microbiology* (Vol. 15, Issue 12, pp. 724–739). Nature Publishing Group. https://doi.org/10.1038/nrmicro.2017.125

Quax, T. E. F., Lucas, S., Reimann, J., Pehau-Arnaudet, G., Prevost, M. C., Forterre, P., Albers, S. V., & Prangishvili, D. (2011). Simple and elegant design of a virion egress structure in Archaea. *Proceedings of the National Academy of Sciences of the United States of America*, *108*(8), 3354–3359. https://doi.org/10.1073/pnas.1018052108

Quemin, E. R. J., Chlanda, P., Sachse, M., Forterre, P., Prangishvili, D., & Krupovic, M. (2016). Eukaryotic-like virus budding in archaea. *MBio*, *7*(5). https://doi.org/10.1128/mBio.01439-16

Quemin, E. R. J., Lucas, S., Daum, B., Quax, T. E. F., Kühlbrandt, W., Forterre, P., Albers, S.-V., Prangishvili, D., & Krupovic, M. (2013). First Insights into the Entry Process of Hyperthermophilic Archaeal Viruses. *Journal of Virology*, *87*(24), 13379–13385. https://doi.org/10.1128/jvi.02742-13

Rössler, N., Klein, R., Scholz, H., & Witte, A. (2004). Inversion within the haloalkaliphilic virus ϕCh1 DNA results in differential expression of structural proteins. *Molecular Microbiology*, *52*(2), 413–426. https://doi.org/10.1111/j.1365-2958.2003.03983.x

Schülein, M. (2019). Construction of a deletion mutant in ϕCh1; Examination of BgaH activities. Bachelorarbeit

Stan-Lotter, H., & Fendrihan, S. (2015). Halophilic archaea: Life with desiccation, radiation and oligotrophy over geological times. *Life*, *5*(3), 1487–1496. https://doi.org/10.3390/life5031487

Svirskaitė, J., Oksanen, H. M., Daugelavičius, R., & Bamford, D. H. (2016). Monitoring physiological changes in haloarchaeal cell during virus release. *Viruses*, *8*(3). https://doi.org/10.3390/v8030059

Tang, S. L., Nuttall, S., & Dyall-Smith, M. (2004). Haloviruses HF1 and HF2: Evidence for a Recent and Large Recombination Event. *Journal of Bacteriology*, *186*(9), 2810–2817. https://doi.org/10.1128/JB.186.9.2810-2817.2004

Tindall, B., Mills, A., & Grant, W. (1980). An Alkalophilic Red Halophilic Bacterium with a Low Magnesium Requirement from a Kenyan Soda Lake. In *Journal of General Microbiology* (Vol. 116).

Tomkins, J. (2015). Information Processing Differences Between Archaea and Eukaraya-Implications for Homologs and the Myth of Eukaryogenesis. *Answers Research Journal*, *8*, 121–141.
www.answersingenesis.org/arj/v8/archaea_eukaraya_homologs_eukaryogenesis.pdf

Uldahl, K. B., Jensen, S. B., Bhoobalan-Chitty, Y., Martínez-Álvarez, L., Papathanasiou, P., & Peng, X. (2016). Life Cycle Characterization of Sulfolobus Monocaudavirus 1, an Extremophilic Spindle-Shaped Virus with Extracellular Tail Development. *Journal of Virology*, *90*(12), 5693–5699. https://doi.org/10.1128/jvi.00075-16

Valentine, D. L. (2007). Adaptations to energy stress dictate the ecology and evolution of the Archaea. www.nature.com/reviews/micro

Van De Vossenberg, J. L. C. M., Arnold, ·, Driessen, J. M., & Konings, W. N. (1998). *The essence of being extremophilic: the role of the unique archaeal membrane lipids* (Vol. 2). http://www.tigr.org/

Vreeland, R. H. (2012). Advances in understanding the biology of halophilic microorganisms. In *Advances in Understanding the Biology of Halophilic Microorganisms*. Springer Netherlands. https://doi.org/10.1007/978-94-007-5539-0

Witte, A., Baranyi, U., Klein, R., Sulzner, M., Luo, C., Wanner, G., Krüger, D. H., & Lubitz, W. (1997). Characterization of Natronobacterium magadii phage ΦCh1, a unique archaeal phage containing DNA and RNA. *Molecular Microbiology*, *23*(3), 603–616. https://doi.org/10.1046/j.1365-2958.1997.d01-1879.x

Woese, C. R., Kandlert, O., & Wheelis, M. L. (1990). Towards a natural system of organisms: Proposal for the domains Archaea, Bacteria, and Eucarya (Euryarchaeota/Crenarchaeota/kingdom/evolution). In *Proc. Nati. Acad. Sci. USA* (Vol. 87).

Zhou, M., Xiang, H., Sun, C., & Tan, H. (2004). Construction of a novel shuttle vector based on an RCR-plasmid from a haloalkaliphilic archaeon and transformation into other haloarchaea. In *Biotechnology Letters* (Vol. 26).